HHS Public Access

Author manuscript

Neuron. Author manuscript; available in PMC 2018 March 08.

Published in final edited form as:

Neuron. 2017 March 08; 93(5): 1110–1125.e5. doi:10.1016/j.neuron.2017.01.029.

SoxC transcription factors promote contralateral retinal ganglion cell differentiation and axon guidance in the mouse visual system

Takaaki Kuwajima[1,*], **Célia A. Soares**[1], **Austen A. Sitko**[2], **Véronique Lefebvre**[4], and **Carol Mason**[1,2,3,**]

[1]Department of Pathology and Cell Biology, College of Physicians and Surgeons, Columbia University, New York, New York 10032

[2]Department of Neuroscience, College of Physicians and Surgeons, Columbia University, New York, New York 10032

[3]Department of Ophthalmology, College of Physicians and Surgeons, Columbia University, New York, New York 10032

[4]Department of Cell Biology, and Orthopaedic and Rheumatologic Research Center, Cleveland Clinic Lerner Research Institute, Cleveland, Ohio 44195

Summary

Transcription factors control cell identity by regulating diverse developmental steps such as differentiation and axon guidance. The mammalian binocular visual circuit is comprised of projections of retinal ganglion cells (RGCs) to ipsilateral and contralateral targets in the brain. A transcriptional code for ipsilateral RGC identity has been identified, but less is known about the transcriptional regulation of contralateral RGC development. Here we demonstrate that SoxC genes (*Sox4, 11*, and *12*) act on the progenitor-to-postmitotic transition to implement contralateral, but not ipsilateral, RGC differentiation, by binding to Hes5 and thus repressing Notch signaling. When SoxC genes are deleted in postmitotic RGCs, contralateral RGC axons grow poorly on chiasm cells *in vitro*, project ipsilaterally at the chiasm midline *in vivo*, and Plexin-A1 and Nr-CAM expression in RGCs is downregulated. These data implicate SoxC transcription factors in the regulation of contralateral RGC differentiation and axon guidance.

[*]Corresponding author (tk2288@columbia.edu). [**]Corresponding author and Lead contact (cam4@columbia.edu).

Author contributions: Conceptualization, T.K. and C.M.; Methodology, T.K. and C.M.; Validation, C.A.S. and A.A.S.; Formal Analysis, T.K.; Investigation, T.K.; Resources, V.L. and C.M.; Writing – Original Draft, T.K. and C.M.; Writing – Review & Editing, T.K., C.A.S., A.A.S., V. L. and C.M.; Visualization, T.K.; Supervision, C.M.; Project Administration, T.K. and C.M.; Funding Acquisition, V.L. and C.M.;

Introduction

During the development of neural circuits, axons are guided to their targets in the brain by molecular cues along their paths. The expression of axonal receptors that respond to such guidance cues at distinct points along pathways is regulated by transcriptional mechanisms (Butler and Tear, 2007; Jessell, 2000; Polleux et al., 2007). As such, specific transcription factors (TFs) establish cell subtype identity through shaping molecular programs for axon guidance.

Retinal ganglion cell (RGC) axon pathway choice at the optic chiasm midline to project ipsilaterally or contralaterally is key to establishing the binocular visual circuit in mammals. Ipsilateral RGCs arise from the ventrotemporal (VT) retina and contralateral RGCs from retinal regions outside of the VT sector (non-VT) from embryonic day (E) 14 to E17, and from the VT retina from E17.5 to postnatal day 0 (P0) (Erskine and Herrera, 2014; Petros et al., 2008).

The molecular pathways underlying the ipsilateral retinal projection are known for the mouse visual system. The guidance receptor EphB1 is upregulated in VT RGCs that project ipsilaterally from E14 to E17, and interacts with its ligand ephrin-B2 on radial glial cells at the optic chiasm, leading to the formation of the ipsilateral projection (Petros et al., 2009; Williams et al., 2003). The zinc finger TF Zic2 governs ipsilateral RGC identity and drives expression of EphB1 and the serotonin transporter (Sert), that functions in activity-dependent refinement in thalamic and midbrain targets in VT RGCs (Garcia-Frigola et al., 2008; Garcia-Frigola and Herrera, 2010; Herrera et al., 2003; Lee et al., 2008).

Guidance receptors mediating the contralateral retinal projection have been identified. Plexin-A1 and Nr-CAM expressed in Zic2-negative RGCs promote contralateral axon outgrowth through interactions with the guidance cues, semaphorin6D and Nr-CAM, which are expressed on midline glia, and with Plexin-A1 on early-born neurons at the optic chiasm midline (Kuwajima et al., 2012; Williams et al., 2006). In addition, the semaphorin receptor Neuropilin1 is expressed in these same RGCs and participates in attracting contralateral axons to the midline by binding to its ligand VEGF at the optic chiasm (Erskine et al., 2011).

To date, only one TF, the LIM homeodomain protein Islet2, regulates contralateral RGC axon guidance (Pak et al., 2004). However, Islet2 is expressed in only ~30% of RGCs in non-VT retina and primarily regulates the late-born contralateral RGC projection that extends from VT retina at E18. The expression pattern and function of Islet2 in RGC axon guidance do not match those of the contralateral RGC guidance receptors identified to date. Therefore, other TFs must exist that direct midline crossing through controlling expression of contralateral RGC-specific guidance receptors.

The 5’ non-coding regions of *Plexna1* (encoding Plexin-A1) and *Nrcam* (encoding neural cell adhesion molecule, Nr-CAM) contain their regulatory sequences (Sanchez-Arrones et al., 2013; Wong et al., 2003). Through an *in silico* search, we found that non-coding regions are conserved across binocular species, and identified the Sox family of TFs, which shares a highly conserved *Sry*-related high-mobility-group DNA-binding domain, as having binding

sites to *Plexna1* and *Nrcam*. Within this family, the SoxC genes (Sox4, Sox11, and Sox12) are expressed in developing RGCs (Hoser et al., 2008; Jiang et al., 2013; Usui et al., 2013). Moreover, expression of Plexin-A1 is downregulated in *Sox4*-depleted cancer cells (Huang et al., 2012). Sox4 and Sox11 regulate corticospinal neuron trajectory by activating *Fezf2* expression via binding to enhancer elements conserved among vertebrates (Shim et al., 2012). Therefore, we considered the SoxC TFs as good candidates for regulating expression of *Plxna1* and *Nrcam* and thus the contralateral RGC axon trajectory at the optic chiasm midline.

Sox4 and Sox11 function in retinal morphogenesis and RGC neurogenesis beginning at E11, and *Sox4/Sox11* conditional mutant mice display a severe hypoplasia of the developing retina, leading to a reduced size of the retina and thinner RGC and inner plexiform layers in the adult retina (Jiang et al., 2013; Usui et al., 2013). However, whether SoxC TFs are expressed in all or a subset of RGCs (e.g., ipsi- vs. contralaterally-projecting), whether they direct differentiation of these RGCs, and whether SoxC TFs play a role in axon guidance at the optic chiasm midline, were not known.

Here we examine the expression and role of SoxC (Sox4, 11, and 12) TFs in RGC differentiation and axon guidance at the chiasm midline. We show that SoxC genes are highly expressed in RGCs in regions of the retina where contralateral RGCs reside, from E13.5 onward. Further, we identify a novel transcriptional pathway involving the SoxC TFs in regulating contralateral RGC differentiation and guidance post-differentiation.

Results

SoxC genes are expressed in contralateral but not ipsilateral RGCs

To relate SoxC expression to the spatial and temporal aspects of the formation of the ipsi- and contralateral RGC projections, we examined expression patterns of SoxC genes (*Sox4, Sox11,* and *Sox12*) in the retina at the three phases of RGC axon extension during optic chiasm formation: E12 – 13.5 when the first RGCs extend from central retina both contralaterally and transiently, ipsilaterally (Soares and Mason, 2015), E14 – E17 when the permanent ipsilaterally-projecting RGCs extend from the VT retina and contralaterally projecting RGCs from non-VT retina, and E17.5 - P0, when contralaterally projecting RGCs extend from VT as well as non-VT retina (Figure 1A) (Petros et al., 2008). *Sox4*, *Sox11,* and *Sox12* mRNAs are highly expressed in the central retina at E13.5, and by E14.5 in RGCs in more peripheral regions of the retina, excluding VT retina (Figure 1A). After E17.5, SoxC mRNA expression extends into VT retina, where late-born contralateral RGCs are situated (Figure 1A). Ki67 and Islet1/2 are markers for progenitors and mature RGCs, respectively (Bhansali et al., 2014; Pan et al., 2008; Usui et al., 2013). At E14.5, SoxC genes are expressed in differentiated, Islet1/2^{+} RGCs, but are absent from Ki67^{+} progenitors (Figure 1B).

From E14 onwards, the transcription factor Zic2 is expressed in VT RGCs that project ipsilaterally (Herrera et al., 2003). In situ hybridization for SoxC TFs and immunohistochemistry for Zic2 was performed in alternate (Figure 1C) or the same sections (Figures 1D and S1A). At E15.5 and E18.5, the majority of SoxC TFs-positive RGCs lack

Zic2. However, at the border of the VT region where Zic2 is highly expressed and adjacent to the SoxC TFs-expressing zone, a few RGCs weakly express both Zic2 and *Sox4*: In a 200 μm x 200 μm region of VT retina, 4.3% (1.8 / 42.6 cells) and 7.9% (5 / 63.1 cells) of Sox4-positive cells express Zic2 at E15.5 and E18.5, respectively ; n = 3 embryos at each age (Figures 1D and S1A). Moreover, at E15.5, SoxC TFs are expressed by RGCs expressing the contralateral RGC receptor *Plexin-A1* in non-VT, e.g. dorsotemporal (DT) retina, where contralateral RGCs arise, but not in VT retina where Plexin-A1 is absent at this stage (Figure 1E). These data establish that SoxC genes are expressed predominantly in RGCs that project contralaterally, suggesting that SoxC TFs may have a selective role in contralateral RGC development.

SoxC TFs regulate contralateral but not ipsilateral RGC differentiation

We next investigated how *Sox4*, *Sox11*, and *Sox12* function in RGC development by deletion of these genes in $Sox4^{flox/flox}Sox11^{flox/flox}Sox12^{-/-}$ ($Sox4^{f/f}Sox11^{f/f}Sox12^{-/-}$) triple conditional mutant embryos at E14.5, when ipsilateral and contralateral RGCs are spatially segregated into VT and non-VT retina, respectively. We electroporated *Cre* recombinase plasmid into the $Sox4^{f/f}Sox11^{f/f}Sox12^{-/-}$ contralateral retina *ex vivo* to delete *Sox4* and *Sox11*, with constitutive deletion of *Sox12*, as $Sox12^{-/-}$ single mutant mice are viable after birth and develop normally (Bhattaram et al., 2010) (Figure 2).

We next examined whether SoxC TFs differentially affect maturation of contralateral (DT) and ipsilateral (VT) retinal cells (Figures 2A–D). *CAG-GFP* and *CAG-Cre* plasmids were electroporated *ex vivo* into E14.5 WT or $Sox4^{f/f}Sox11^{f/f}Sox12^{-/-}$ DT retina to generate WT or $Sox4^{-/-}Sox11^{-/-}Sox12^{-/-}$ GFP^+ cells, respectively, and *CAG-GFP* alone into $Sox4^{f/f}Sox11^{f/f}Sox12^{-/-}$ retina to generate $Sox12^{-/-}$ GFP^+ cells. After culturing the entire retina for 24 hours, retinae were dissociated into a single-cell suspension, plated, and kept *in vitro* for 48 hours to allow electroporated GFP^+ retinal precursors to differentiate into RGCs (Figures S2A–D). 95.6 ± 0.7% of GFP^+ cells express Cre (>300 of total GFP^+ cells counted, n = 3 cultures). Cultures of $Sox4^{-/-}Sox11^{-/-}Sox12^{-/-}$ DT retinal cells contained fewer $Islet1/2^+/GFP^+$ cells and more $Ki67^+/GFP^+$ cells compared with WT or $Sox12^{-/-}$ DT retinal cell cultures (Figures 2A–D). Brn3a is a marker for RGCs, especially contralateral RGCs (Quina et al., 2005). Fewer $Sox4^{-/-}Sox11^{-/-}Sox12^{-/-}$ DT retinal cells expressed Brn3a compared with WT cells ($Brn3a^+/GFP^+$ cells in WT = 60.2% ± 4.2 vs $Sox4^{-/-}Sox11^{-/-}Sox12^{-/-}$ = 8.1% ± 2.5, >300 of total GFP^+ cells counted for each condition, n = 3 cultures, $P<0.001$, Student's t test) (data not shown). In contrast, $Sox4^{-/-}Sox11^{-/-}Sox12^{-/-}$ VT GFP^+ retinal cells displayed little alteration of the number of differentiated RGCs vs progenitor cells, similar to WT or $Sox12^{-/-}$ VT retinal cells (Figures 2A–D). These data thus suggest that SoxC TFs are required for contralateral but not ipsilateral RGC differentiation.

Since $Sox12^{-/-}$ DT retina differentiate into postmitotic RGCs as in WT retina (Figures 2C–D), we investigated the overlapping function of SoxC TFs in RGC differentiation (Figure 2E). $Sox4^{-/-}Sox11^{-/-}Sox12^{-/-}$ triple mutant DT cultures had the fewest $Islet1/2^+/GFP^+$ cells compared with WT, $Sox4^{-/-}$ or $Sox11^{-/-}$ single, or $Sox4^{-/-}Sox11^{-/-}$, $Sox4^{-/-}Sox12^{-/-}$

or *Sox11*$^{-/-}$*Sox12*$^{-/-}$ double mutants. Thus, SoxC TFs similarly regulate the differentiation of contralateral RGCs.

We next asked whether SoxC TFs regulate RGC differentiation as cells transit from progenitor to postmitotic neuron and/or maintain the postmitotic differentiation state, by deleting SoxC genes at different times. To delete SoxC genes with temporal control, we utilized *CAG-ER*^{T2}*CreER*^{T2} and administered 4-hydroxytamoxifen (4OHT) to dissociated retinal cell cultures to elicit *Cre*/*loxP*-mediated recombination, reported to occur within 24 hours in the retina *in vivo* (Matsuda and Cepko, 2007) and within 12 hours *in vitro* (data not shown). *CAG-GFP* and *CAG-ER*^{T2}*CreER*^{T2} plasmids were co-electroporated into E14.5 *Sox4*$^{f/f}$*Sox11*$^{f/f}$*Sox12*$^{-/-}$ DT retina, and *Sox4*$^{-/-}$*Sox11*$^{-/-}$*Sox12*$^{-/-}$ DT GFP$^+$ cells or *Sox12*$^{-/-}$ GFP$^+$ cells were generated with or without adding 4OHT to the medium, respectively (Figure 2F). 94.8 ± 0.8% of GFP$^+$ cells in dissociated retinal cell culture express Cre in the nucleus after incubation with 4OHT for 24 hours (>300 of total GFP$^+$ cells counted, n = 3 cultures) (data not shown). 4OHT addition to dissociated retinal cell cultures at 12 hrs, at the transition point between the progenitor state and differentiation produced cultures of *Sox4*$^{-/-}$*Sox11*$^{-/-}$*Sox12*$^{-/-}$ DT retinal cells (Figure S2). Fewer Islet1/2$^+$/GFP$^+$ cells and more Ki67$^+$/GFP$^+$ cells were observed compared with cultures without 4OHT (Figures 2G–I). However, when 4OHT was applied to dissociated retinal cells at 48 hrs, at the time when most cells are postmitotic (Figure S2), *Sox4*$^{-/-}$*Sox11*$^{-/-}$*Sox12*$^{-/-}$ and *Sox12*$^{-/-}$ DT retinal cell cultures had a similar number of Islet1/2$^+$ cells and Ki67$^+$ cells (Figures 2G–I). Apoptotic features such as nuclear fragmentation and DNA condensation were not detected in more than 95% of *Sox4*$^{-/-}$*Sox11*$^{-/-}$*Sox12*$^{-/-}$ and *Sox12*$^{-/-}$ DT GFP$^+$ retinal cells (*Sox4*$^{-/-}$*Sox11*$^{-/-}$*Sox12*$^{-/-}$ = 4.9 ± 1.0 vs *Sox12*$^{-/-}$ = 3.6 ± 1.1, n = 4 cultures, N.S., Student's t test) (data not shown). These data suggest that SoxC TFs regulate contralateral RGC differentiation at the transition between progenitor and early postmitotic state but that these TFs do not affect the RGC post-differentiation state or survival.

SoxC TFs promote contralateral RGC differentiation by antagonizing Notch-Hes5 signaling

Notch-Hes5 signaling is important for driving proliferation in the chick retina and mouse cerebral cortex (Nelson et al., 2006; Tiberi et al., 2012), and in the hippocampus, the *Hes5* gene is a direct target of Sox21, which regulates hippocampal adult neurogenesis (Matsuda et al., 2012). Thus, we asked whether SoxC TFs might regulate contralateral RGC differentiation by antagonizing Notch-Hes5 signaling.

First, we examined expression patterns of *Hes5* and *Notch1* genes in the developing retina (Figures 3A and S3). *Hes5* is expressed in Ki67$^+$ progenitor cells in the neuroblastic layer but not in the ciliary marginal zone (CMZ) which is a source of RGCs (Marcucci et al., 2016; Wang et al., 2016). *Notch1* is also highly expressed in the neuroblastic layer and moderately expressed in the RGC layer. In contrast, *Sox4* is expressed in Islet1/2$^+$ postmitotic RGCs. These data suggest that *Hes5* and SoxC genes have complementary expression in the developing retina.

Second, we investigated whether SoxC TFs modulate Notch-regulated transcriptional activity of the *Hes5* promoter, which contains binding sites both for Sox TFs and the Notch1

intracellular domain (NICD) (Matsuda et al., 2012). Whereas NICD alone upregulated reporter activity of the *Hes5* promoter, Sox4, Sox11, and Sox12 antagonized this Notch-driven transcriptional activation (Figure 3B). To investigate functional antagonistic interactions of SoxC TFs with Notch-Hes5 signaling in RGC differentiation, we next tested whether overexpression of Hes5 inhibits contralateral RGC differentiation (Figures 3C–E). E14.5 WT DT retina was co-electroporated with *CAG-GFP* and *CAG-Hes5* plasmids: Overexpression of Hes5 led to a decrease in Islet1/2$^+$/GFP$^+$ cells and an increase in Ki67$^+$/GFP$^+$ cells. In contrast, overexpression of Hes5 in *Sox4*$^{-/-}$*Sox11*$^{-/-}$*Sox12*$^{-/-}$ mutant DT retina did not change the number of Ki67$^+$/GFP$^+$ cells compared to *Sox4*$^{-/-}$*Sox11*$^{-/-}$*Sox12*$^{-/-}$ mutant DT cells. However, after overexpression of Hes5 in VT retina, VT RGC differentiation was unaffected (Figures S4A–B). These results suggest that defects in contralateral RGC differentiation are induced by loss-of-function of SoxC genes and gain-of-function of Hes5 in the retina.

DAPT, an inhibitor of the gamma-secretase complex, blocks Notch activity and reduces Hes5 expression levels, and promotes RGC differentiation in developing mouse and chick retina (Nelson et al., 2006; Nelson et al., 2007). To investigate whether defects in RGC differentiation in SoxC mutants could be rescued by repressing Notch activity with DAPT, *Sox4*$^{-/-}$*Sox11*$^{-/-}$*Sox12*$^{-/-}$ GFP$^+$ cells were cultured in the presence of DAPT (Figures 3F–H). The reduced number of Islet1/2$^+$/GFP$^+$ cells and the increased number of Ki67$^+$/GFP$^+$ cells observed in *Sox4*$^{-/-}$*Sox11*$^{-/-}$*Sox12*$^{-/-}$ DT retinal cells were restored to WT levels by DAPT. VT retinal cells from WT and *Sox4*$^{-/-}$*Sox11*$^{-/-}$*Sox12*$^{-/-}$ mutant retinae were not affected by DAPT addition (Figures S4C–D).

To further examine whether the Notch pathway, especially Hes5, is specifically involved in RGC differentiation defects in *Sox4*$^{-/-}$*Sox11*$^{-/-}$*Sox12*$^{-/-}$ retinal cells, we analyzed expression levels of *Hes5*, *Hes1* and *Ccnd1* (encoding CyclinD1) mRNAs, the latter two genes important for maintaining the retinal progenitor state and preventing RGC differentiation (Das et al., 2009; Nelson et al., 2006; Ohtsuka et al., 1999). After electroporation of *CAG-GFP* and *CAG-Cre* plasmids, cells from the WT or *Sox4*$^{-/-}$*Sox11*$^{-/-}$*Sox12*$^{-/-}$ GFP$^+$ region of the DT retina were cultured for 48 hours, and expression levels measured by qPCR. *Hes5* mRNA is the most upregulated gene (1.96-fold activation) among these three genes in SoxC mutant retinal cells (Figure 3I).

Taken together, these data suggest that Notch-Hes5 signaling maintains the progenitor state in cells in the regions of the retina giving rise to contralaterally-projecting RGCs, and that reduced activity of Notch-Hes5 signaling can rescue defects in *Sox4*$^{-/-}$*Sox11*$^{-/-}$*Sox12*$^{-/-}$ mutant RGC differentiation.

SoxC mutants display defects in contralateral RGC differentiation *in vivo*

To investigate the function of SoxC TFs *in vivo*, *CAG-GFP* alone or *CAG-GFP* and *CAG-Cre* plasmids were electroporated into the retina of WT or *Sox4*$^{f/f}$*Sox11*$^{f/f}$*Sox12*$^{-/-}$ mice at E14.5, to generate WT, *Sox12*$^{-/-}$ or *Sox4*$^{-/-}$*Sox11*$^{-/-}$*Sox12*$^{-/-}$ GFP$^+$ cells (Figure 4A). 92.4 ± 0.3% of GFP$^+$ cells expressed Cre at E18.5 (>350 of total GFP$^+$ cells counted, n = 3 embryos). We then analyzed the number of Islet1/2$^+$ RGCs or Ki67$^+$ progenitor cells at E18.5 (Figure 4B). In both WT and *Sox12*$^{-/-}$ retinas, ~50% of GFP$^+$ cells expressed Islet1/2

and ~20% of GFP$^+$ cells expressed Ki67. In contrast, in *Sox4*$^{-/-}$*Sox11*$^{-/-}$*Sox12*$^{-/-}$ retinas, only 11% of GFP$^+$ cells expressed Islet1/2 and ~60% of GFP$^+$ cells expressed Ki67, and the latter cells were positioned in the progenitor cell layer (Figures 4B–D). These data suggest that SoxC TFs can influence contralateral RGC differentiation *in vivo*.

SoxC mutant contralateral RGC axon outgrowth is impaired on chiasm cells

Although SoxC TFs appear to be necessary for contralateral RGC differentiation, it remains unclear whether SoxC TFs might also mediate axon outgrowth and guidance at the chiasm midline. To do this, we employed two experimental strategies to manipulate SoxC expression in RGCs without perturbing RGC differentiation.

Defects in RGC differentiation in SoxC mutant DT retina were attenuated by DAPT, which blocks Notch signaling as shown above, and only then could long axons be detected (Figures 3F–H). We therefore analyzed GFP$^+$ axon outgrowth in culture with or without chiasm cells in the presence or absence of DAPT (Figures S5A–C). Without chiasm cells, *Sox4*$^{-/-}$*Sox11*$^{-/-}$*Sox12*$^{-/-}$ GFP$^+$ DT retinal explants display fewer GFP$^+$ axons than WT or *Sox12*$^{-/-}$ GFP$^+$ DT explants, while treatment with DAPT led to robust GFP$^+$ axon outgrowth of *Sox4*$^{-/-}$*Sox11*$^{-/-}$*Sox12*$^{-/-}$ GFP$^+$ DT explants. However, in the presence of chiasm cells, even with addition of DAPT, axon outgrowth of *Sox4*$^{-/-}$*Sox11*$^{-/-}$*Sox12*$^{-/-}$ GFP$^+$ DT explants was poor (Figures S5B–C). In contrast, *Sox4*$^{-/-}$*Sox11*$^{-/-}$*Sox12*$^{-/-}$ and WT GFP$^+$ VT retinal explants displayed similar GFP$^+$ axon outgrowth with and without chiasm cells (Figures S6A–B). Therefore, this experiment indicates that blocking Notch signaling can rescue differentiation and axon outgrowth in SoxC mutant RGCs when on laminin, but not when they are on chiasm cells (Figures S5B–C). These data suggest that SoxC TFs are necessary to regulate axon outgrowth on chiasm cells independent of Notch signaling, potentially via other pathways regulating guidance receptors.

Next, we designed an experiment to conditionally delete SoxC genes and analyze axon outgrowth on chiasm cells without perturbing Notch signaling. Since deletion of SoxC genes in postmitotic RGCs *in vitro* does not perturb RGC differentiation and neurites can extend (Figures 2F–I), we electroporated *CAG-GFP* and *CAG-ER*^{T2}*CreER*^{T2} plasmids into E14.5 *Sox4*$^{f/f}$*Sox11*$^{f/f}$*Sox12*$^{-/-}$ DT retina, and then added 4OHT to generate *Sox4*$^{-/-}$*Sox11*$^{-/-}$*Sox12*$^{-/-}$ GFP$^+$ DT explants cultured on laminin alone or on chiasm cells after axons had extended (Figures 5B). *Sox4*$^{-/-}$*Sox11*$^{-/-}$*Sox12*$^{-/-}$ GFP$^+$ DT retinal explants displayed robust GFP$^+$ axon outgrowth on laminin without chiasm cells as did WT and *Sox12*$^{-/-}$ GFP$^+$ DT explants. However, *Sox4*$^{-/-}$*Sox11*$^{-/-}$*Sox12*$^{-/-}$ GFP$^+$ DT retinal explants grown on chiasm cells showed a large reduction in axon outgrowth compared with WT and *Sox12*$^{-/-}$ DT explants (Figures 5C–D). These data suggest that even if axons can extend, SoxC TFs are required for contralateral RGC outgrowth on chiasm cells, potentially by regulating guidance receptors on RGCs needed to respond to signals from chiasm cells.

Midline crossing of contralateral retinal axons at the optic chiasm is impaired in SoxC mutants *in vivo*

First, we investigated effects of SoxC TFs on axon outgrowth at E18.5 *in vivo* by deletion of SoxC genes at the transition between progenitor and postmitotic state by electroporation of

CAG-GFP and *CAG-Cre* plasmids into $Sox4^{f/f}Sox11^{f/f}Sox12^{-/-}$ at E14.5. SoxC mutant GFP^+ cells remained in the progenitor zone below the RGC layer (Figure 4), and few axons extended into the optic nerve and into the optic chiasm (Figure S7).

We next examined a role for SoxC TFs in retinal axon guidance at the optic chiasm midline *in vivo* by deleting SoxC genes with greater temporal control. E14.5 $Sox4^{f/f}Sox11^{f/f}Sox12^{-/-}$ non-VT retina were electroporated *in utero* with *CAG-GFP* and $CAG\text{-}ER^{T2}CreER^{T2}$ plasmids, and then injected i.p. with 4OHT at E16.5 to delete SoxC genes in the electroporated RGCs. At the time of 4OHT injection, ~40% of GFP^+ cells in the WT and Sox mutant retina are $Islet1/2^+$ RGCs, and the axons of these cells project into the optic nerve but not as far as the optic chiasm (data not shown). When *CAG-GFP* and $CAG\text{-}ER^{T2}CreER^{T2}$ plasmids were co-electroporated together at E14.5 and 4OHT was injected at E16 and were examined at E18.5, 93.6 ± 1.0% of GFP^+ cells express Cre in nucleus (>350 of total GFP^+ cells counted, n = 3 embryos). We then analyzed the number of $Islet1/2^+$ RGCs and $Ki67^+$ progenitor cells in $Sox4^{-/-}Sox11^{-/-}Sox12^{-/-}$ retina at E18.5 (two days post-4OHT injection) (Figures 6A–C). In both WT and $Sox4^{-/-}Sox11^{-/-}Sox12^{-/-}$ embryos, ~60% of GFP cells express Islet1/2 and ~12% of GFP cells express Ki67, indicating that mutant and WT retinae have differentiated similarly (Figures 6B–C).

Next, we analyzed axon projections in WT and $Sox4^{-/-}Sox11^{-/-}Sox12^{-/-}$ RGCs at the optic chiasm midline at E18.5 (Figures 6D–E). The cells in central retina in both WT and mutant retina were electroporated and thus almost all GFP^+ axons in WT embryos projected contralaterally. In contrast, in $Sox4^{-/-}Sox11^{-/-}Sox12^{-/-}$ mice, GFP^+ RGC axons elelctroporated also in central retina, projected ipsilaterally and contralaterally (Figure 6D). As indicated by the ipsilateral index analysis, a five-fold increase in the proportion of GFP^+ axons projecting ipsilaterally was observed in $Sox4^{-/-}Sox11^{-/-}Sox12^{-/-}$ mice compared with WT or $Sox12^{-/-}$ mice (Figure 6E).

We also examined whether $Sox4^{-/-}Sox11^{-/-}Sox12^{-/-}$ mutant contralateral and ipsilateral axons reach the superior colliculus (SC) and dorsal lateral geniculate nucleus (dLGN) compared with WT axons, at E18.5 (Figure S8). Both WT and $Sox4^{-/-}Sox11^{-/-}Sox12^{-/-}$ contralateral axons reached the borders of the SC and dLGN. In the WT, a few ipsilateral axons could be detected at or near the chiasm midline (Figure 6D), but few were noted as far as the dLGN or SC (Figure S8). In contrast, in $Sox4^{-/-}Sox11^{-/-}Sox12^{-/-}$ mice, numerous ipsilateral axons were detected in the optic chiasm (Figure 6D) and in the optic tract outside the dLGN and the SC (Figure S8). As seen in the WT at E18 (Soares and Mason, 2015), few axons from the central retinal RGCs penetrate these targets. Taken together, deletion of SoxC genes in postmitotic RGCs led to an increased ipsilateral projection, and these axons reach the borders of their targets in dLGN and SC. These data suggest that SoxC factors play a role in contralateral RGC differentiation as well as axon guidance at the optic chiasm midline.

SoxC TFs regulate Plexin-A1 and NrCAM expression in RGCs

Two possible molecular mechanisms could explain the aberrant projection of central retinal RGC axons ipsilaterally in SoxC mutants in which the SoxC TFs were ablated at E16.5-E18.5. First, axon guidance receptors in contralateral RGCs such as Plexin-A1, Nr-CAM,

and Neuropilin1 (Erskine et al., 2011; Kuwajima et al., 2012), could be downregulated in the absence of SoxC genes. Alternatively (or in addition), the ipsilateral transcription factor Zic2, and/or the ipsilateral axon guidance receptor EphB1 (Herrera et al., 2003; Williams et al., 2003) could be ectopically induced in RGCs in the absence of SoxC TFs. We therefore examined the expression of *Plexin-A1*, *Nr-CAM*, *Neuropilin1*, and *EphB1* mRNA, and Zic2 protein in E18.5 *Sox4*$^{-/-}$*Sox11*$^{-/-}$*Sox12*$^{-/-}$ retina *in vivo* after *in utero* electroporation of *CAG-GFP* and *CAG-ER*^{T2}*CreER*^{T2} at E14.5 and treatment with 4OHT at E16 (Figures 7A–B). *Sox4*$^{-/-}$*Sox11*$^{-/-}$*Sox12*$^{-/-}$ GFP^{+} RGCs failed to express *Plexin-A1* and *Nr-CAM* mRNAs compared to WT GFP^{+} cells, although *Neuropilin1* mRNA was detected in SoxC mutant cells (Figure 7A). Zic2 protein and *EphB1* mRNA were not ectopically induced in *Sox4*$^{-/-}$*Sox11*$^{-/-}$*Sox12*$^{-/-}$ GFP^{+} RGCs in non-VT retina (Figure 7B).

We next examined whether *Plexna1* (encoding Plexin-A1) and *Nrcam* (encoding Nr-CAM) are direct targets of SoxC TFs (Figures 7C–F). We searched for conserved regions among binocular species within the 5' non-coding regions (−1 ~ -5000) of *Plexna1* and *Nrcam* using UCSC Genome Browser and found that putative regulatory non-coding regions of *Plexna1* and *Nrcam*, which contain pan-Sox binding sites, C(T/A)TTG(T/A)(T/A) using TESS and PROMO (Bhattaram et al., 2010; Messeguer et al., 2002; Schug, 2008). We made luciferase-based reporter constructs containing Sox binding sites for *Plexna1* and *Nrcam* non-coding regions (Figure 7C), and examined whether SoxC TFs modulate transcriptional activity of the *Plexna1* and *Nrcam* promoter in HEK293 cells (Figure 7D) and in SoxC mutant DT retinal cells *in vitro* (Figure 7E). Ectopic expression of SoxC TFs upregulated transcriptional activity of both promoters in HEK293 cells (Figure 7D). Endogenous SoxC TFs upregulate the transcriptional activity of *Plexna1* and *Nrcam* promoters in 3-day cultures compared to 1-day cultures of WT DT retina. In contrast, transcriptional activation of neither promoter could be detected in 3-day DT culture after deletion of SoxC genes in postmitotic RGCs. The activity was slightly elevated in 3-day cultures of WT VT retina (Figure 7E).

Finally, binding of SoxC TFs to *Plexna1* and *Nrcam* promoters was analyzed by chromatin immunoprecipitation (ChIP) (Figure 7F). An enrichment of predicted DNA on *Plexna1* and *Nrcam* promoters was detected with anti-FLAG antibody after electroporation of FLAG-tagged Sox4, FLAG-tagged Sox11 or FLAG-tagged Sox12 construct into DT retina compared with control IgG or FLAG-antibody after electroporation of empty vector.

Together, these data indicate that SoxC TFs bind to the promoters of *Plexna1* and *Nrcam* and regulate their expression, in contralateral RGCs.

Discussion

Mechanisms of contralateral RGC growth and guidance during formation of the binocular visual circuit, are poorly understood compared with the directives for ipsilateral RGC growth and guidance. Through an *in silico* search, we identified the SoxC transcription factors as candidate TFs that direct the contralateral RGC projection during optic chiasm formation, specifically, through their regulation of their RGC differentiation and of their axon guidance receptors Plexin-A1 and Nr-CAM. In this study, inactivation of SoxC TFs at

two specific time points in RGC development, i.e., during RGC proliferation and axon guidance, allowed us to reveal a dual function of SoxC TFs that actively contributes to contralateral RGC differentiation and growth at the optic chiasm (Figure 8).

SoxC TFs regulate differentiation of RGCs that project contralaterally

TFs crucial for RGC cell fate specification have been identified (Wang and Harris, 2005; Xiang, 2013). The subsequent differentiation of postmitotic RGCs is mediated by various TFs in monocular and binocular species (Kanekar et al., 1997; Wu et al., 2015). However, TFs selectively mediating contralateral or ipsilateral RGC cell fate and differentiation were not identified. Our study demonstrates that SoxC TFs are necessary for contralateral RGC differentiation at the transition between progenitor and the early postmitotic state (Figures 2 and 4), but RGCs in VT retina during the period of ipsilateral RGC genesis from E14 - E17 do not appear to require SoxC TFs. However, from E17.5 - P0, SoxC genes are expressed within VT retina, where contralateral RGCs also reside in this late period, implying that SoxC TFs may also mediate later-born contralateral RGC differentiation from E17.5.

SoxC TFs stimulate contralateral RGC differentiation by antagonizing the Notch signaling pathway

Notch, and its downstream effector, the bHLH transcription factor Hes, are important for retinal morphogenesis, progenitor cell maintenance, cell fate determination and specification in the retina (Bao and Cepko, 1997; Henrique et al., 1997; Jadhav et al., 2006; Maurer et al., 2014; Mizeracka et al., 2013; Nelson et al., 2006; Ohtsuka et al., 1999). Sox4 and Sox11 regulate neuronal differentiation in the developing cortex through regulating their targets NeuroD1 and Tbr2 (Chen et al., 2015). Our study is the first to show that the Notch1-Hes5 signaling pathway is important for maintaining the progenitor state specifically of contralateral retinal progenitors and that antagonistic interactions between Notch-Hes5 and SoxC TFs influence the balance between cell proliferation and RGC differentiation in regions of the retina giving rise to contralateral RGCs (Figure 3).

The individual SoxC TFs are not functionally equivalent: Sox11 and 12 strongly antagonize Notch-induced transcriptional activity of Hes5, but Sox4 only moderately antagonizes Notch activity, although *Sox4*$^{-/-}$ and *Sox11*$^{-/-}$ single mutant retina shows more severe defects in RGC differentiation than *Sox12*$^{-/-}$ retina, which displays normal RGC differentiation (Figures 2C–D). In fact, *Sox4*$^{-/-}$*Sox11*$^{-/-}$*Sox12*$^{-/-}$ triple mutant DT retina has fewer RGCs than in the *Sox4*$^{-/-}$ or *Sox11*$^{-/-}$ single mutant or *Sox4*$^{-/-}$*Sox11*$^{-/-}$ double mutants (Figure 2E). In other systems, *Sox4*$^{-/-}$*Sox11*$^{-/-}$*Sox12*$^{-/-}$ triple mutants have a thinner neural tube compared with *Sox4*$^{-/-}$*Sox11*$^{-/-}$ mutants (Bhattaram et al., 2010). Loss of function in *Sox12*$^{-/-}$ retina might be compensated through increased expression of *Sox4* and *Sox11* in the retina, as previously shown in the brain and spinal cord (Hoser et al., 2008). Therefore, loss of *Sox12* function could be compensated by upregulation of Sox4 and 11 expression and/or enrichment of Sox4 and 11 on the target promoter region.

SoxC TFs and Hes5 do not appear to be involved in ipsilateral RGC differentiation, even though they are expressed in progenitors in VT retina (Figures 2C, S3 and S4). How is proliferation and differentiation of ipsilateral RGCs which are situated in VT retina,

regulated? Most recently, we have identified Cyclin D2 as a regulator of cell cycle progression and exit in VT retina during the production of $Zic2^+$ RGCs (Marcucci et al., 2016; Wang et al., 2016). As overexpression of Hes5 in VT retina has no effect on RGC differentiation, contralateral and ipsilateral RGC differentiation may be mediated by distinct molecules and/or downstream signals of Hes5.

Regulation of the contralateral RGC projection by SoxC TFs is independent of Zic2

How are the contralateral and ipsilateral retinal projection encoded in binocular species? TFs responsible for contralateral RGC specification might suppress expression of TFs for ipsilateral RGC specification, or vice versa. SoxC TFs show complementary expression patterns to those of Zic2, but Zic2 expression was not detected in SoxC-deficient RGCs (Figure 7B). Moreover, overexpression of Zic2 in contralateral retina does not affect RGC differentiation and axon outgrowth (Garcia-Frigola et al., 2008). These data suggest that SoxC TFs does not affect Zic2 expression (Figure 7).

Interestingly, loss of Islet2, which is normally expressed in a subset of contralateral RGCs, leads to an increased number of $Zic2^+$ RGCs in VT retina, and a concomitantly increased ipsilateral projection (Pak et al., 2004). Taken together, while a Islet2-Zic2 cross repression appears to participate in the designation of ipsilateral and contralateral RGCs, SoxC TFs do not engage with the Zic2 pathway during binocular visual circuit formation (Figure 8).

Transcriptional code for the contralateral RGC projection: SoxC TFs regulate axon guidance receptor expression

TFs selectively regulate expression of axon guidance receptors and ligands, and contribute to proper neural connectivity in the nervous system (Butler and Tear, 2007; Erskine and Herrera, 2014; Polleux et al., 2007). Our study has shown SoxC TFs bind to the promoter regions of *Plexna1* and *Nrcam* and regulate their expression levels in contralateral retina (Figure 7). While *Nr-CAM*$^{-/-}$ and *Islet2*$^{-/-}$ single mutants display the same defects in the contralateral projection at E18 - P0 (Pak et al., 2004; Williams et al., 2006), Islet2 fails to activate transcriptional activities of *Nrcam* promoter regions including Islet2 binding sites by luciferase reporter assay (data not shown).

What molecular mechanisms lead to an induction of an ipsilateral projection from non-VT retina in $SoxC^{-/-}$ embryos? Plexin-A1 and Nr-CAM expressed in contralateral RGCs serve as receptors for semaphorin6D, Plexin-A1 and Nr-CAM which are expressed at the optic chiasm midline and facilitate contralateral RGC axon midline crossing (Kuwajima et al., 2012). Therefore, downregulation of functional receptors, Plexin-A1 and Nr-CAM in $SoxC^{-/-}$ mutant retina may lead to a reduction in retinal axon outgrowth in response to growth-permissive signals from chiasm cells (Figure 6). Moreover, the inhibitory chiasmatic environment would stimulate $SoxC^{-/-}$ mutant RGC axons from central retina to avoid the midline, leading to an increase in ipsilateral axons extending to the LGN and SC (Figure S8). However, the maintenance of the contralateral projection in SoxC mutant RGC axons may be due to the continued expression of *Neuropilin1* (Erskine et al., 2011) (Figure 7A). Thus, depletion of *Neuropilin1* in SoxC mutant contralateral retina would be predicted to lead to additional increased ipsilateral projection in SoxC mutants. Moreover, *Cre-loxP*

recombination in the electroporated RGCs could have occurred after many of their axons had passed through the chiasm.

In summary, we have elucidated the function of SoxC TFs in RGCs that project contralaterally, through controlling distinct targets for their differentiation and axon guidance. Further investigation is needed to determine whether SoxC TFs control expression of these target genes for RGC differentiation and axon guidance simultaneously, or sequentially, whether SoxC TFs are also involved in more distal phases, in axon targeting and RGC axon regeneration, and how the regulation of ipsilateral RGC differentiation intersects with contralateral RGC differentiation.

STAR METHODS

CONTACT FOR REAGENT AND RESOURCE SHARING

Further information and requests for reagents should be directed to and will be fulfilled by Lead Contact, Carol Mason (cam4@columbia.edu).

EXPERIMENTAL MODEL AND SUBJECT DETAILS

Animals

All animal experiments were performed according to the regulatory guidelines of the Columbia University Institutional Animal Care and Use Committee. Generation of *Sox4*$^{flox/flox}$ mutant mice (strain background; 129SvEx:C57BL/6) has previously been described (Penzo-Mendez et al., 2007). Generation of *Sox11*$^{flox/flox}$, *Sox12*$^{-/-}$ and *Sox4*$^{flox/flox}$*Sox11*$^{flox/flox}$*Sox12*$^{-/-}$ mutants (strain background; 129SvEx:C57BL/6) has previously been described (Bhattaram et al., 2010). The triple mutant mice were obtained from the colony of Véronique Lefebvre, Cleveland Clinic, and maintained at Columbia University. Breeding of *Sox4*$^{flox/flox}$*Sox11*$^{flox/flox}$*Sox12*$^{-/-}$ mice produced embryos of the same genotype, which were used in all *in vivo* and culture experiments. C57BL/6 wild type embryos were used as a negative control. Single, double, or triple SoxC mutants for the *in vitro* analysis in Figure 2E were generated by breeding heterozygous *Sox4*$^{f/+}$*Sox11*$^{f/+}$*Sox12*$^{-/+}$ mice, which are the offspring of *Sox4*$^{flox/flox}$*Sox11*$^{flox/flox}$*Sox12*$^{-/-}$ and C57BL/6 wild type mice. Genotyping of each embryo was carried out by PCR for *Sox4*$^{+}$ or *Sox4*^{flox} allele-specific segments with the primers FP: 5'-GAAGGAGGCGGAGAGTAGACG G- 3', and RP: 5'-CATAGCTCAACACAAATGCCAACG C- 3', for *Sox11*$^{+}$ or *Sox11*^{flox} allele-specific segments with the primers FPA: 5'-TTCGTGATTGCAACAAAGGCGGAG- 3' and RPA: 5'-GCTCCCTGCAGTTTAAGAAATCGG- 3', and for *Sox12*$^{+}$ allele with the primers FPA: 5'-CCTTCTTGCGCATGCTTGATGCTT- 3'and RP: 5'-GGAAATCAAGTTTCCGGCGACCAA- 3' and for the *Sox12*$^{-}$ allele with the primers FPB: 5'-ATGCAAATGCTGAGTTCTCTGCCC- 3' and RP (Bhattaram et al., 2010; Penzo-Mendez et al., 2007). The latter mice are born at roughly Mendelian ratios, are fertile, and survive to adulthood.

All mice were housed in a pathogen-free barrier facility in static polysulfone microisolator cages, up to 5 mice per cage, on autoclaved ALPHA-dri/Cob Blend bedding, at a

temperature of 68 – 79°F and 30 – 70% humidity. Mice were maintained in a 12 h light/dark cycle with acidified water (pH 2.5 – 3.0) and irradiated pelleted diet provided *ad libitum*. Noon of the day on which a vaginal plug was found was considered E0.5.

The total number of embryos and retinal cultures analyzed for *in vivo* and *in vitro* experiments, respectively, from >3 independent rounds of electroporation was indicated in each figure legend, and the procedures were described in METHOD DETAILS. Embryos were randomly chosen for *ex vivo* and *in utero* electroporation, immunostaining and *in situ* hybridization in each experiment and condition, and these embryos were assigned to each experimental group.

METHOD DETAILS

In situ hybridization and Immunohistochemistry

In situ hybridization with DIG-labeled probes for Sox4, 11, 12 (gifts of V. Lefebvre) (Dy et al., 2008), Notch1 (Reaume et al., 1992), Hes5 (gift of R. Kageyama, Kyoto University, Japan) (Akazawa et al., 1992), EphB1 (Williams et al., 2003), Plexin-A1, Neuropilin1, Nr-CAM (Williams et al., 2006; Yoshida et al., 2006), was performed on 12 μm brain or retinal sections as described previously (Williams et al., 2003). Fluorescent Sox4 mRNA was detected with HNPP fluorescent detection kit (Sigma). The number of Sox4 mRNA$^+$ cells expressing Zic2 was counted in a 200 μm x 200 μm area at the border of the VT region adjacent to the SoxC-expressing zone in 3 cryosections including 6 retinal sections caudal to the section with optic nerve, and the number of cells was averaged for each embryo (n = 1). The analysis was repeated in 3 embryos. Immunolabeling was performed with the following primary antibodies: Rabbit IgG anti-GFP (1:500, Thermo Fisher), chick IgG anti-GFP (1:500, Thermo Fisher), mouse IgG anti-Islet1/2 (1:50) (anti-Islet1/2 antibody, was raised against Islet1 expressed in almost all RGCs, and also recognizes Islet2 expressed in a subset of RGCs and co-expressed with Islet1 (Bhansali et al., 2014; Pan et al., 2008; Tsuchida et al., 1994)) and anti-neurofilament (2H3; 1:5; gifts of S. Morton and T. Jessell, Columbia University) (Dodd et al., 1988), mouse anti-Brn3a (1:500, EMD Millipore), rabbit IgG anti-Ki67 (1:500, EMD Millipore), rabbit anti-Zic2 (1:5000; gift of S. Brown, Columbia University) (Brown et al., 2003), mouse anti-Cre (1:200, Abcam). Cy3 (1:500, Jackson) or AlexFluor488 (1:500, Thermo Fisher) were used as secondary antibodies. Hoechst 33258 (1:1000, Thermo Fisher) was used for nuclear staining. Images were captured by a Zeiss Axioplan 2 microscope with an Axiocam digital camera. 300 μm of thick vibratome sections, as in Figure 6D, were imaged on a Zeiss AxioImager M2 microscope with Apotome, AxioCam MRm camera, Neurolucida software (V11.06, MicroBrightField Systems) after immunostaining with GFP and clearing sections with *Clear*^{T2} (Kuwajima et al., 2013).

Electroporation

In utero and *ex vivo* electroporation were performed as previously described (Garcia-Frigola et al., 2007; Matsuda and Cepko, 2007; Petros et al., 2009) with minor modifications. 0.3 - 0.5 μl of DNA solution of *CAG-GFP* (0.5 μg/μl) with *CAG-Cre* or *CAG-ER*^{T2}*CreER*^{T2} (2.0 μg/μl) (gifts of C. Cepko, Harvard University, Addgene plasmids #13775 and #13777)

(Matsuda and Cepko, 2007) and/or *CAG-Hes5* (2.0 μg/μl) (gift of R. Kageyama, Kyoto University, Japan) plus 0.03% Fast Green Dye was injected into the subretinal space for *in utero* or peripheral dorsotemporal (DT) or ventrotemporal (VT) retina for *ex vivo* electroporation of E14.5 embryos. The "+" electrode of tweezer-type electrodes (CUY650-P7, Nepa Gene) were positioned on the injected eye, and the "- " electrode on the opposite side of the head for *in utero* electroporation. The "+" electrode was positioned on the ventral and dorsal surface of the head for *ex vivo* electroporation of DT or VT retina. In both types of electroporation 50 ms square current pulses were delivered at 45 V and 950 ms intervals by an electroporator (CUY21EDIT Square Wave, Nepa Gene).

Retinal cell cultures and analysis

For dissociated retinal cell cultures, after *ex vivo* electroporation, the lens and vasculature were removed and the intact retinal cup was cultured in DMEM/F12 serum-free medium for 24 hours. The eye cup was then dissociated, plated at a density of 70,000 cells in 35 mm glass-bottomed culture dishes, with a 14 mm microwell (MatTek Corp.) coated with poly-L-ornithine (Sigma) and laminin (Thermo Fisher) in DMEM/F12 serum-free medium containing 0.4% methylcellulose (Sigma). Dissociated retinal cells were fixed for 20 min with 4% PFA. For quantification in dissociated retinal cultures of Islet1/2$^+$ and Ki67$^+$, and in later experiments, of Cre$^+$ or Brn3a$^+$/GFP$^+$ cells (%), for each experiment, 5 electroporated eye cups were pooled, dissociated, and divided into 2 wells for the analysis. For Figure 2E, 2 electroporated eye cups from each embryo with a different genotype were used for the analysis. In all of these cases, the number of GFP$^+$ cells that were also Islet1/2$^+$, Ki67$^+$, Cre$^+$ or Brn3a$^+$ cells was counted in 5 areas (500 μm x 650 μm /each), in the center and at 12, 3, 6, 9 o'clock in each well, and these numbers were summed and averaged (n = 1 experiment). 3–5 independent rounds of such cultures were repeated for each condition.

For retinal explant cultures, after *ex vivo* electroporation and culture of electroporated retinal eye cup for 24 hours, GFP$^+$ DT or VT retinal explants were cultured on poly-L-ornithine- and laminin-coated microwell dishes with or without dissociated chiasm cells plated a density of 70,000 cells/dish as described previously (Kuwajima et al., 2012; Wang et al., 1996). For quantification of GFP$^+$ neurite outgrowth in explant cultures, the total area covered by neurites of individual explants was quantified by measuring pixel intensity with ImageJ software. Each experiment was carried out three times, and within each experiment, at least five explants, each from a different embryo/retina were treated in each experimental group. Explants with GFP$^+$ neurites extending from only one region, or explants with few or no axons, independent of the condition, were excluded from quantitative analysis. 4OHT (final concentration, 1 μM) (Sigma) or DAPT (final concentration, 10 μM) (Sigma) were added into the both cultures at specific times depending on experimental design.

In vivo analysis

Combinations of DNA plasmids were *in utero* electroporated into E14.5 retina and embryos were fixed at E18.5. For Figures 6, 7 and S8, 1mg of 4OHT (Sigma) diluted in corn oil (Sigma) was intraperitoneally injected into pregnant mothers carrying E16 embryos after electroporation at E14.5. For quantification of Islet1/2$^+$ or Ki67$^+$/GFP$^+$ cells (%) in 12 μm cryosections, all GFP$^+$ cells were found only in non-VT retina *in vivo*. The number of GFP$^+$

cells that were Islet1/2$^+$, Ki67$^+$ or Cre$^+$ was counted in 3–5 retinal sections, with the middle section at the level of the optic nerve, the numbers were summed, and then percent of GFP$^+$ that were either Islet1/2$^+$ or Ki67$^+$/GFP$^+$ calculated per embryo (n = 1). For each condition, 3–5 embryos from independent individual rounds of *in utero* electroporation were analyzed. For quantification of retinal decussation of GFP$^+$ axons at the optic chiasm, the average pixel intensity of GFP$^+$ RGC axons in the ipsilateral and contralateral optic tracts in two adjacent sections just caudal to the optic chiasm as shown in Figure 6E, was measured with ImageJ software. The ipsilateral index was obtained by dividing the intensity of the ipsilateral projection by the sum of the contralateral and ipsilateral pixel intensities per embryo (n = 1). For each condition, 4–6 embryos from independent rounds of *in utero* electroporation were analyzed. The ipsilateral index obtained in mutants was normalized to that in WT embryos. For quantification of GFP$^+$ RGC axon outgrowth in Figure S7, three 20 μm cryosections just rostral to the chiasm, and the subsequent three sections through the optic chiasm were analyzed. The pixel intensity of GFP$^+$ axons within the optic nerve and at the optic chiasm was measured by ImageJ software and the total pixel intensity from the sections of nerve and of chiasm was calculated. The average pixel intensity in these two locations was divided by the total number of GFP$^+$ cells (electroporated) in the retina to give a GFP$^+$ axon outgrowth index per embryo. For each condition, 3–4 embryos from independent rounds of *in utero* electroporation were analyzed. Data obtained in mutants was normalized to WT.

Luciferase assay

FLAG-Sox4, *Sox11*, or *Sox12* (Dy et al., 2008) was transfected into HEK293 cells or *CAG-GFP* and *CAG-ER^{T2}CreER^{T2}* were electroporated *ex vivo* into DT or VT retina along with *Hes5* (−2767 to −2244 bp) (gift of Dr. H. Okano, Keio University) (Matsuda et al., 2012), *Plexna1* (−3085 to −2386 bp) or *Nrcam* (-1001 to +15 bp) luciferase reporter constructs (pGL3-*Hes5*, pGL4.10-*Plexna1*, or pGL4.10-*Nrcam*), a *Renilla* luciferase construct (Promega). For the Hes5 reporter assay, the Notch1 intracellular domain (NICD) was also transfected in HEK293 cells. Firefly luciferase activity was measured 48 hours after transfection in HEK293 cells or 24 or 72 hours in cultured retinal cells dissociated as above using Dual-Luciferase Reporter Assay system (Promega).

ChIP assay

After *ex vivo* electroporation of 0.5 μl of *FLAG-Sox4*, *Sox11*, or *Sox12* or control vector (2.0 μg/μl) and *CAG-GFP* (0.5 μg/μl) into DT retina, whole retina was cultured for 72 hours. 30 GFP$^+$ retinae were cross-linked in 1% formaldehyde in PBS for 10 min at room temperature and used for ChIP assay for each condition, as previously described (Kurita et al., 2006). FLAG-Sox4, Sox11 or Sox12 protein was immunoprecipitated with mouse IgG anti-FLAG or non-immune IgG as a control. qPCR was performed with the following primers: *Plexna1* promoter (120 bp; Forward: 5'-GTCCACAACCATAAGGCTCCA- 3', Reverse: 5'-GCTCTCTCCCAACTCTGAGTAACA- 3'), *Nrcam* promoter (100 bp; Forward: 5'-GGTTTCTGAAAAACAACCAGGA- 3', Reverse: 5'-AAGGTGCCCATCTTCCTGTC- 3').

qRT-PCR

After *ex vivo* electroporation of *CAG-GFP* and *CAG-Cre* plasmids into E14.5 WT or $Sox4^{f/f}Sox11^{f/f}Sox12^{-/-}$ DT retina, cells from the GFP^+ region of the retina were cultured for 48 hours. For total RNA preparation, cells were lysed and RNA was isolated using RNA isolation kit (Thermo Fisher). RNA (100 ng) was reversed transcribed to cDNA. Quantitative PCR was performed in duplicate using Power SybrGreen Mix (Applied Biosystems) and Realplex 4 Mastercycler PCR System (Eppendorf). Results are presented as linearized Ct values normalized to *Gapdh* gene. The results of qRT-PCR in SoxC mutants were normalized to the mean value of WT for each experiment, and experiments were repeated 4 times. Primers for qPCR were previously described: *Hes5* Forward: 5'-AAGAGCCTGCACCAGGACTA- 3', Reverse: 5'-CGCTGGAAGTGGTAAAGCA- 3') (Tiberi et al., 2012), *Hes1* (Forward: 5'-TCTGACCACAGAAAGTCATCA- 3', Reverse: 5'-AGCTATCTTTCTTAAGTGCATC- 3') (Tiberi et al., 2012), *Ccnd1* (Forward: 5'-TGCCATCCATGCGGAAA- 3', Reverse: 5'-AGCGGGAAGAACTCCTCTTC- 3') (Kothapalli et al., 2007) and *Gapdh* (Forward 5'-TGACCACAGTCCATGCCATC-3':, Reverse: 5'-CATACCAGGAAATGAGCTTGAC- 3') (Usui et al., 2013).

QUANTIFICATION AND STATISTICAL ANALYSIS

All data were analyzed and graphs were constructed using Image J, Microsoft Excel and GraphPad Prism 6 software. All error bars represent the standard error of the mean (SEM), and statistical analysis was determined using unpaired two-tailed Student's t test or one-way ANOVA, two-way ANOVA or three-way ANOVA followed by the Tukey's post hoc test, as indicated in the figure legends associated with each figure. *p<0.05, **p<0.01, ***p<0.001, N.S. Not significant (p>0.05).

Supplementary Material

Refer to Web version on PubMed Central for supplementary material.

Acknowledgments

We thank Jane Dodd, Florencia Marcucci, Takeshi Sakurai, and members of the Mason lab for helpful comments on the experiments and manuscript, and Mika Melikyan for mouse breeding. We are grateful to Hideyuki Okano for *Notch1* cDNA construct and *Hes5*-luciferase reporter construct, Goichi Miyoshi and Ryoichiro Kageyama for *Hes5* cDNA constructs for *in situ* hybridization and expression in mammalian cells, and Connie Cepko for *CAG-Cre* and $CAG\text{-}ER^{T2}CreER^{T2}$; Susan Morton and Tom Jessell for Islet1/2 and neurofilament antibodies and Stephen Brown for Zic2 antibody. This work was supported by National Institutes of Health grants EY015290 (CM), AR46249 and AR60016 (VL).

References

Akazawa C, Sasai Y, Nakanishi S, Kageyama R. Molecular characterization of a rat negative regulator with a basic helix-loop-helix structure predominantly expressed in the developing nervous system. The Journal of biological chemistry. 1992; 267:21879–21885. [PubMed: 1400497]

Bao ZZ, Cepko CL. The expression and function of Notch pathway genes in the developing rat eye. J Neurosci. 1997; 17:1425–1434. [PubMed: 9006984]

Bhansali P, Rayport I, Rebsam A, Mason C. Delayed neurogenesis leads to altered specification of ventrotemporal retinal ganglion cells in albino mice. Neural development. 2014; 9:11. [PubMed: 24885435]

Bhattaram P, Penzo-Mendez A, Sock E, Colmenares C, Kaneko KJ, Vassilev A, Depamphilis ML, Wegner M, Lefebvre V. Organogenesis relies on SoxC transcription factors for the survival of neural and mesenchymal progenitors. Nature communications. 2010; 1:9.

Brown LY, Kottmann AH, Brown S. Immunolocalization of Zic2 expression in the developing mouse forebrain. Gene Expression Patterns. 2003; 3:361–367. [PubMed: 12799086]

Butler SJ, Tear G. Getting axons onto the right path: the role of transcription factors in axon guidance. Development. 2007; 134:439–448. [PubMed: 17185317]

Chen C, Lee GA, Pourmorady A, Sock E, Donoghue MJ. Orchestration of Neuronal Differentiation and Progenitor Pool Expansion in the Developing Cortex by SoxC Genes. J Neurosci. 2015; 35:10629–10642. [PubMed: 26203155]

Das G, Choi Y, Sicinski P, Levine EM. Cyclin D1 fine-tunes the neurogenic output of embryonic retinal progenitor cells. Neural development. 2009; 4:15. [PubMed: 19416500]

Dodd J, Morton SB, Karagogeos D, Yamamoto M, Jessell TM. Spatial regulation of axonal glycoprotein expression on subsets of embryonic spinal neurons. Neuron. 1988; 1:105–116. [PubMed: 3272160]

Dy P, Penzo-Mendez A, Wang H, Pedraza CE, Macklin WB, Lefebvre V. The three SoxC proteins--Sox4, Sox11 and Sox12--exhibit overlapping expression patterns and molecular properties. Nucleic acids research. 2008; 36:3101–3117. [PubMed: 18403418]

Erskine L, Herrera E. Connecting the Retina to the Brain. Asn Neuro. 2014:6.

Erskine L, Reijntjes S, Pratt T, Denti L, Schwarz Q, Vieira JM, Alakakone B, Shewan D, Ruhrberg C. VEGF Signaling through Neuropilin 1 Guides Commissural Axon Crossing at the Optic Chiasm. Neuron. 2011; 70:951–965. [PubMed: 21658587]

Fabre PJ, Shimogori T, Charron F. Segregation of ipsilateral retinal ganglion cell axons at the optic chiasm requires the Shh receptor Boc. J Neurosci. 2010; 30:266–275. [PubMed: 20053908]

Garcia-Frigola C, Carreres MI, Vegar C, Herrera E. Gene delivery into mouse retinal ganglion cells by in utero electroporation. BMC Dev Biol. 2007; 7:103. [PubMed: 17875204]

Garcia-Frigola C, Carreres MI, Vegar C, Mason C, Herrera E. Zic2 promotes axonal divergence at the optic chiasm midline by EphB1-dependent and -independent mechanisms. Development. 2008; 135:1833–1841. [PubMed: 18417618]

Garcia-Frigola C, Herrera E. Zic2 regulates the expression of Sert to modulate eye-specific refinement at the visual targets. EMBO J. 2010

Henrique D, Hirsinger E, Adam J, Le Roux I, Pourquie O, Ish-Horowicz D, Lewis J. Maintenance of neuroepithelial progenitor cells by Delta-Notch signalling in the embryonic chick retina. Curr Biol. 1997; 7:661–670. [PubMed: 9285721]

Herrera E, Brown L, Aruga J, Rachel RA, Dolen G, Mikoshiba K, Brown S, Mason CA. Zic2 patterns binocular vision by specifying the uncrossed retinal projection. Cell. 2003; 114:545–557. [PubMed: 13678579]

Hoser M, Potzner MR, Koch JM, Bosl MR, Wegner M, Sock E. Sox12 deletion in the mouse reveals nonreciprocal redundancy with the related Sox4 and Sox11 transcription factors. Molecular and cellular biology. 2008; 28:4675–4687. [PubMed: 18505825]

Huang HY, Cheng YY, Liao WC, Tien YW, Yang CH, Hsu SM, Huang PH. SOX4 transcriptionally regulates multiple SEMA3/plexin family members and promotes tumor growth in pancreatic cancer. PLoS One. 2012; 7:e48637. [PubMed: 23251334]

Jadhav AP, Cho SH, Cepko CL. Notch activity permits retinal cells to progress through multiple progenitor states and acquire a stem cell property. Proc Natl Acad Sci U S A. 2006; 103:18998–19003. [PubMed: 17148603]

Jessell TM. Neuronal specification in the spinal cord: inductive signals and transcriptional codes. Nature reviews Genetics. 2000; 1:20–29.

Jiang Y, Ding Q, Xie X, Libby RT, Lefebvre V, Gan L. Transcription factors SOX4 and SOX11 function redundantly to regulate the development of mouse retinal ganglion cells. The Journal of biological chemistry. 2013; 288:18429–18438. [PubMed: 23649630]

Kanekar S, Perron M, Dorsky R, Harris WA, Jan LY, Jan YN, Vetter ML. Xath5 participates in a network of bHLH genes in the developing Xenopus retina. Neuron. 1997; 19:981–994. [PubMed: 9390513]

Kothapalli D, Zhao L, Hawthorne EA, Cheng Y, Lee E, Pure E, Assoian RK. Hyaluronan and CD44 antagonize mitogen-dependent cyclin D1 expression in mesenchymal cells. The Journal of cell biology. 2007; 176:535–544. [PubMed: 17296798]

Kurita M, Kuwajima T, Nishimura I, Yoshikawa K. Necdin downregulates CDC2 expression to attenuate neuronal apoptosis. J Neurosci. 2006; 26:12003–12013. [PubMed: 17108174]

Kuwajima T, Sitko AA, Bhansali P, Jurgens C, Guido W, Mason C. ClearT: a detergent- and solvent-free clearing method for neuronal and non-neuronal tissue. Development. 2013; 140:1364–1368. [PubMed: 23444362]

Kuwajima T, Yoshida Y, Takegahara N, Petros TJ, Kumanogoh A, Jessell TM, Sakurai T, Mason C. Optic chiasm presentation of Semaphorin6D in the context of Plexin-A1 and Nr-CAM promotes retinal axon midline crossing. Neuron. 2012; 74:676–690. [PubMed: 22632726]

Lee R, Petros TJ, Mason CA. Zic2 regulates retinal ganglion cell axon avoidance of ephrinB2 through inducing expression of the guidance receptor EphB1. J Neurosci. 2008; 28:5910–5919. [PubMed: 18524895]

Marcucci F, Murcia-Belmonte V, Wang Q, Coca Y, Ferreiro-Galve S, Kuwajima T, Khalid S, Ross ME, Mason C, Herrera E. The Ciliary Margin Zone of the Mammalian Retina Generates Retinal Ganglion Cells. Cell reports. 2016; 17:3153–3164. [PubMed: 28009286]

Matsuda S, Kuwako K, Okano HJ, Tsutsumi S, Aburatani H, Saga Y, Matsuzaki Y, Akaike A, Sugimoto H, Okano H. Sox21 promotes hippocampal adult neurogenesis via the transcriptional repression of the Hes5 gene. J Neurosci. 2012; 32:12543–12557. [PubMed: 22956844]

Matsuda T, Cepko CL. Controlled expression of transgenes introduced by in vivo electroporation. Proc Natl Acad Sci U S A. 2007; 104:1027–1032. [PubMed: 17209010]

Maurer KA, Riesenberg AN, Brown NL. Notch signaling differentially regulates Atoh7 and Neurog2 in the distal mouse retina. Development. 2014; 141:3243–3254. [PubMed: 25100656]

Messeguer X, Escudero R, Farre D, Nunez O, Martinez J, Alba MM. PROMO: detection of known transcription regulatory elements using species-tailored searches. Bioinformatics. 2002; 18:333–334. [PubMed: 11847087]

Mizeracka K, DeMaso CR, Cepko CL. Notch1 is required in newly postmitotic cells to inhibit the rod photoreceptor fate. Development. 2013; 140:3188–3197. [PubMed: 23824579]

Nelson BR, Gumuscu B, Hartman BH, Reh TA. Notch activity is downregulated just prior to retinal ganglion cell differentiation. Developmental neuroscience. 2006; 28:128–141. [PubMed: 16508310]

Nelson BR, Hartman BH, Georgi SA, Lan MS, Reh TA. Transient inactivation of Notch signaling synchronizes differentiation of neural progenitor cells. Developmental biology. 2007; 304:479–498. [PubMed: 17280659]

Ohtsuka T, Ishibashi M, Gradwohl G, Nakanishi S, Guillemot F, Kageyama R. Hes1 and Hes5 as notch effectors in mammalian neuronal differentiation. EMBO J. 1999; 18:2196–2207. [PubMed: 10205173]

Pak W, Hindges R, Lim YS, Pfaff SL, O'Leary DD. Magnitude of binocular vision controlled by islet-2 repression of a genetic program that specifies laterality of retinal axon pathfinding. Cell. 2004; 119:567–578. [PubMed: 15537545]

Pan L, Deng M, Xie X, Gan L. ISL1 and BRN3B co-regulate the differentiation of murine retinal ganglion cells. Development. 2008; 135:1981–1990. [PubMed: 18434421]

Penzo-Mendez A, Dy P, Pallavi B, Lefebvre V. Generation of mice harboring a Sox4 conditional null allele. Genesis. 2007; 45:776–780. [PubMed: 18064674]

Petros TJ, Rebsam A, Mason CA. Retinal axon growth at the optic chiasm: to cross or not to cross. Annu Rev Neurosci. 2008; 31:295–315. [PubMed: 18558857]

Petros TJ, Shrestha BR, Mason C. Specificity and sufficiency of EphB1 in driving the ipsilateral retinal projection. J Neurosci. 2009; 29:3463–3474. [PubMed: 19295152]

Polleux F, Ince-Dunn G, Ghosh A. Transcriptional regulation of vertebrate axon guidance and synapse formation. Nature reviews Neuroscience. 2007; 8:331–340. [PubMed: 17453014]

Quina LA, Pak W, Lanier J, Banwait P, Gratwick K, Liu Y, Velasquez T, O'Leary DD, Goulding M, Turner EE. Brn3a-expressing retinal ganglion cells project specifically to thalamocortical and collicular visual pathways. J Neurosci. 2005; 25:11595–11604. [PubMed: 16354917]

Reaume AG, Conlon RA, Zirngibl R, Yamaguchi TP, Rossant J. Expression analysis of a Notch homologue in the mouse embryo. Developmental biology. 1992; 154:377–387. [PubMed: 1426644]

Sanchez-Arrones L, Nieto-Lopez F, Sanchez-Camacho C, Carreres MI, Herrera E, Okada A, Bovolenta P. Shh/Boc signaling is required for sustained generation of ipsilateral projecting ganglion cells in the mouse retina. J Neurosci. 2013; 33:8596–8607. [PubMed: 23678105]

Schug J. Using TESS to predict transcription factor binding sites in DNA sequence. Current protocols in bioinformatics / editoral board, Andreas D Baxevanis [et al]. 2008; Chapter 2(Unit 2–6)

Shim S, Kwan KY, Li M, Lefebvre V, Sestan N. Cis-regulatory control of corticospinal system development and evolution. Nature. 2012; 486:74–79. [PubMed: 22678282]

Soares CA, Mason CA. Transient ipsilateral retinal ganglion cell projections to the brain: Extent, targeting, and disappearance. Developmental neurobiology. 2015; 75:1385–1401. [PubMed: 25788284]

Tiberi L, van den Ameele J, Dimidschstein J, Piccirilli J, Gall D, Herpoel A, Bilheu A, Bonnefont J, Iacovino M, Kyba M, et al. BCL6 controls neurogenesis through Sirt1-dependent epigenetic repression of selective Notch targets. Nat Neurosci. 2012; 15:1627–1635. [PubMed: 23160044]

Tsuchida T, Ensini M, Morton SB, Baldassare M, Edlund T, Jessell TM, Pfaff SL. Topographic Organization of Embryonic Motor-Neurons Defined by Expression of Lim Homeobox Genes. Cell. 1994; 79:957–970. [PubMed: 7528105]

Usui A, Mochizuki Y, Iida A, Miyauchi E, Satoh S, Sock E, Nakauchi H, Aburatani H, Murakami A, Wegner M, et al. The early retinal progenitor-expressed gene Sox11 regulates the timing of the differentiation of retinal cells. Development. 2013; 140:740–750. [PubMed: 23318640]

Wang JC, Harris WA. The role of combinational coding by homeodomain and bHLH transcription factors in retinal cell fate specification. Developmental biology. 2005; 285:101–115. [PubMed: 16040025]

Wang LC, Rachel RA, Marcus RC, Mason CA. Chemosuppression of retinal axon growth by the mouse optic chiasm. Neuron. 1996; 17:849–862. [PubMed: 8938118]

Wang Q, Marcucci F, Cerullo I, Mason C. Ipsilateral and Contralateral Retinal Ganglion Cells Express Distinct Genes during Decussation at the Optic Chiasm. eNeuro. 2016:3.

Williams SE, Grumet M, Colman DR, Henkemeyer M, Mason CA, Sakurai T. A role for Nr-CAM in the patterning of binocular visual pathways. Neuron. 2006; 50:535–547. [PubMed: 16701205]

Williams SE, Mann F, Erskine L, Sakurai T, Wei S, Rossi DJ, Gale NW, Holt CE, Mason CA, Henkemeyer M. Ephrin-B2 and EphB1 mediate retinal axon divergence at the optic chiasm. Neuron. 2003; 39:919–935. [PubMed: 12971893]

Wong AW, Brickey WJ, Taxman DJ, van Deventer HW, Reed W, Gao JX, Zheng P, Liu Y, Li P, Blum JS, et al. CIITA-regulated plexin-A1 affects T-cell-dendritic cell interactions. Nat Immunol. 2003; 4:891–898. [PubMed: 12910265]

Wu F, Kaczynski TJ, Sethuramanujam S, Li R, Jain V, Slaughter M, Mu X. Two transcription factors, Pou4f2 and Isl1, are sufficient to specify the retinal ganglion cell fate. Proc Natl Acad Sci U S A. 2015; 112:E1559–1568. [PubMed: 25775587]

Xiang M. Intrinsic control of mammalian retinogenesis. Cellular and molecular life sciences : CMLS. 2013; 70:2519–2532. [PubMed: 23064704]

Yoshida Y, Han B, Mendelsohn M, Jessell TM. PlexinA1 signaling directs the segregation of proprioceptive sensory axons in the developing spinal cord. Neuron. 2006; 52:775–788. [PubMed: 17145500]

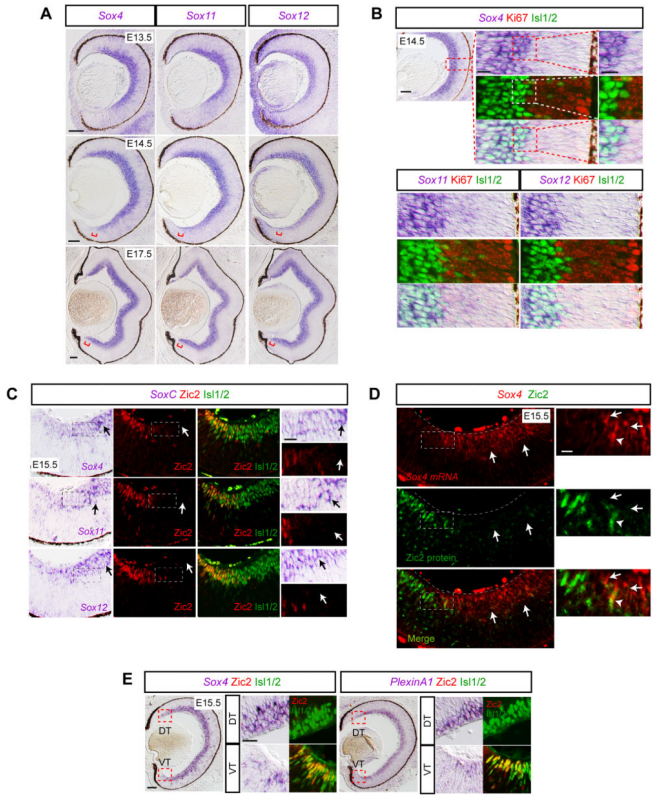

Figure 1. SoxC genes are expressed in regions of the retina giving rise to contralateral RGCs

(A) Expression of *Sox4*, *Sox11,* and *Sox12* mRNAs in the RGC layer at E13.5, E14.5 and E17.5. Red bracket points to VT retina. (B) Expression of *Sox4*, *Sox11,* and *Sox12* mRNAs in RGCs (Islet1/2^{+}), not but in progenitor cells (Ki67^{+}) at E14.5. (C, D) *Sox4*, *Sox11,* and *Sox12* mRNAs are for the most part not co-expressed with Zic2 protein in VT RGCs at E15.5 (arrows), but a few RGCs weakly express both Zic2 and SoxC (arrowheads) in the same section. (E) Similar expression patterns of *Sox4* and *Plexin-A1* mRNAs in DT, but not Zic2^{+} VT, RGCs at E15.5. See also Figure S1. DT, dorsotemporal; VT, ventrotemporal. Scale bars: 100 μm in A, B, E (whole retina); 20 μm in B–E (high magnification of retinal cells).

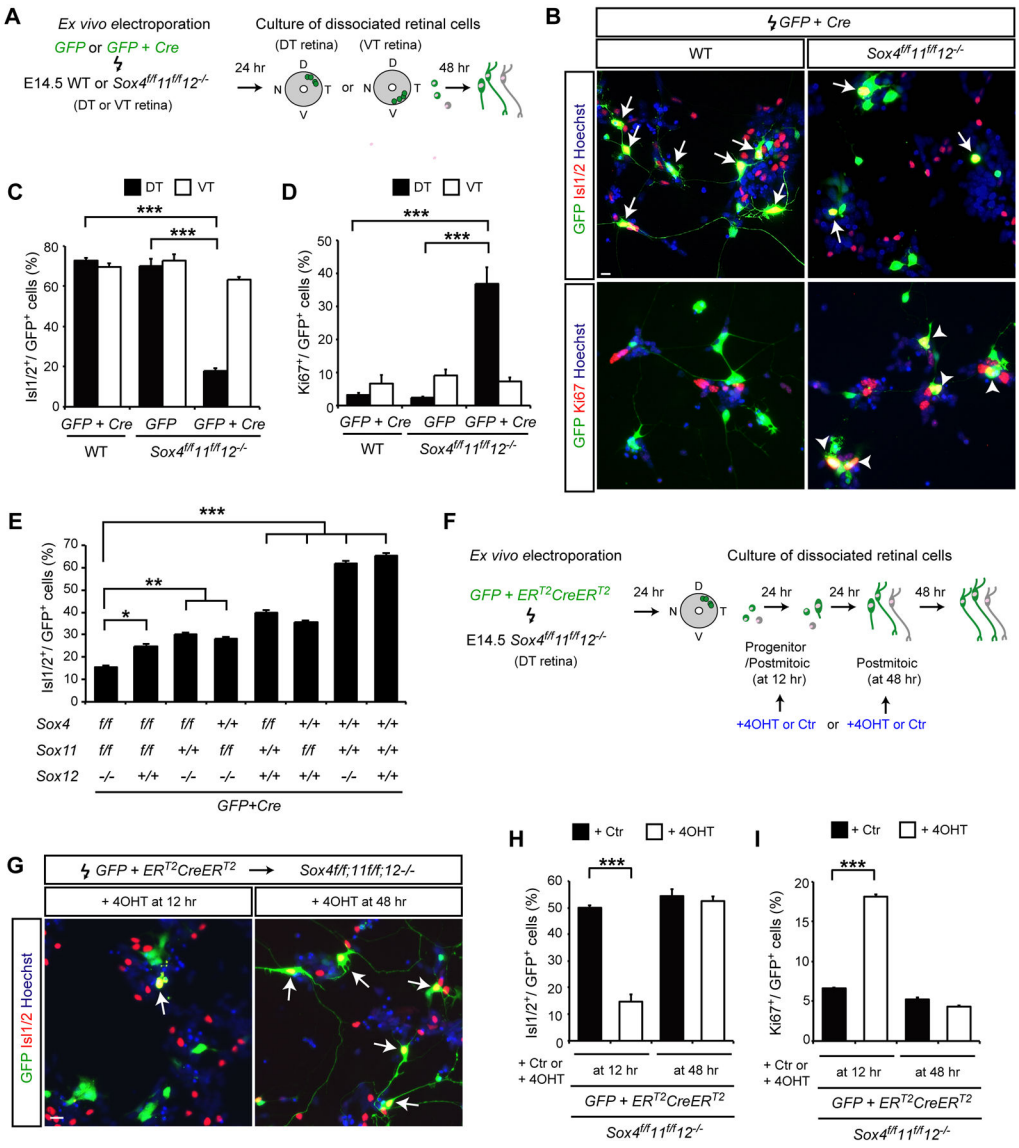

Figure 2. SoxC TFs regulate contralateral but not ipsilateral RGC differentiation

(A) Schema of *ex vivo* electroporation of *CAG-GFP* and *CAG-Cre* plasmids into E14.5 WT or $Sox4^{f/f}Sox11^{f/f}Sox12^{-/-}$ contralateral (DT) or ipsilateral (VT) retina and cell cultures. (B) Representative images of Islet1/2^{+}/GFP^{+} RGCs (arrows) and Ki67^{+}/GFP^{+} progenitor cells (arrowheads) in WT and $Sox4^{-/-}Sox11^{-/-}Sox12^{-/-}$ DT cultures. (C, D) Quantification of Islet1/2^{+}/GFP^{+} cells (%) (C) and Ki67^{+}/GFP^{+} cells (%) (D) in WT, $Sox12^{-/-}$, and $Sox4^{-/-}Sox11^{-/-}Sox12^{-/-}$ DT or VT dissociated cultures (>380 of total GFP^{+} cells counted for each condition, n = 4 – 5, two-way ANOVA). (E) Magnitude of RGC differentiation defects in $Sox4^{-/-}Sox11^{-/-}Sox12^{-/-}$ DT retinal cells compared to WT, SoxC single or double mutant DT retinal cells (>275 of total GFP^{+} cells counted for each condition, n = 3, one-way ANOVA). (F) Schema of *ex vivo* electroporation of both *CAG-GFP* and *CAG-*$ER^{T2}CreER^{T2}$ plasmids into E14.5 $Sox4^{f/f}Sox11^{f/f}Sox12^{-/-}$ DT retina to generate $Sox4^{-/-}Sox11^{-/-}Sox12^{-/-}$ or $Sox12^{-/-}$ GFP^{+} cells during the progenitor/postmitotic state (at

12 hours in dissociated retinal cell cultures) or at the postmitotic state (at 48 hours in dissociated retinal cultures), by adding 4-hydroxytamoxifen (4OHT) or control, ethanol alone (Ctr). (G) Representative images of Islet1/2^{+}/GFP^{+} cells after deletion of SoxC genes at 12 or 48 hours in dissociated retinal cultures (arrows). (H, I) Quantification of Islet1/2^{+}/GFP^{+} cells (%) (H) and Ki67^{+}/GFP^{+} cells (%) (I) from DT retina where all SoxC genes were deleted during the progenitor/postmitotic or at postmitotic state (>510 of total GFP^{+} cells counted for each condition, n = 4, two-way ANOVA). See also Figure S2. DT, dorsotemporal; VT, ventrotemporal. Scale bars: 10 μm. * $p<0.05$, ** $p<0.01$, *** $p<0.001$.

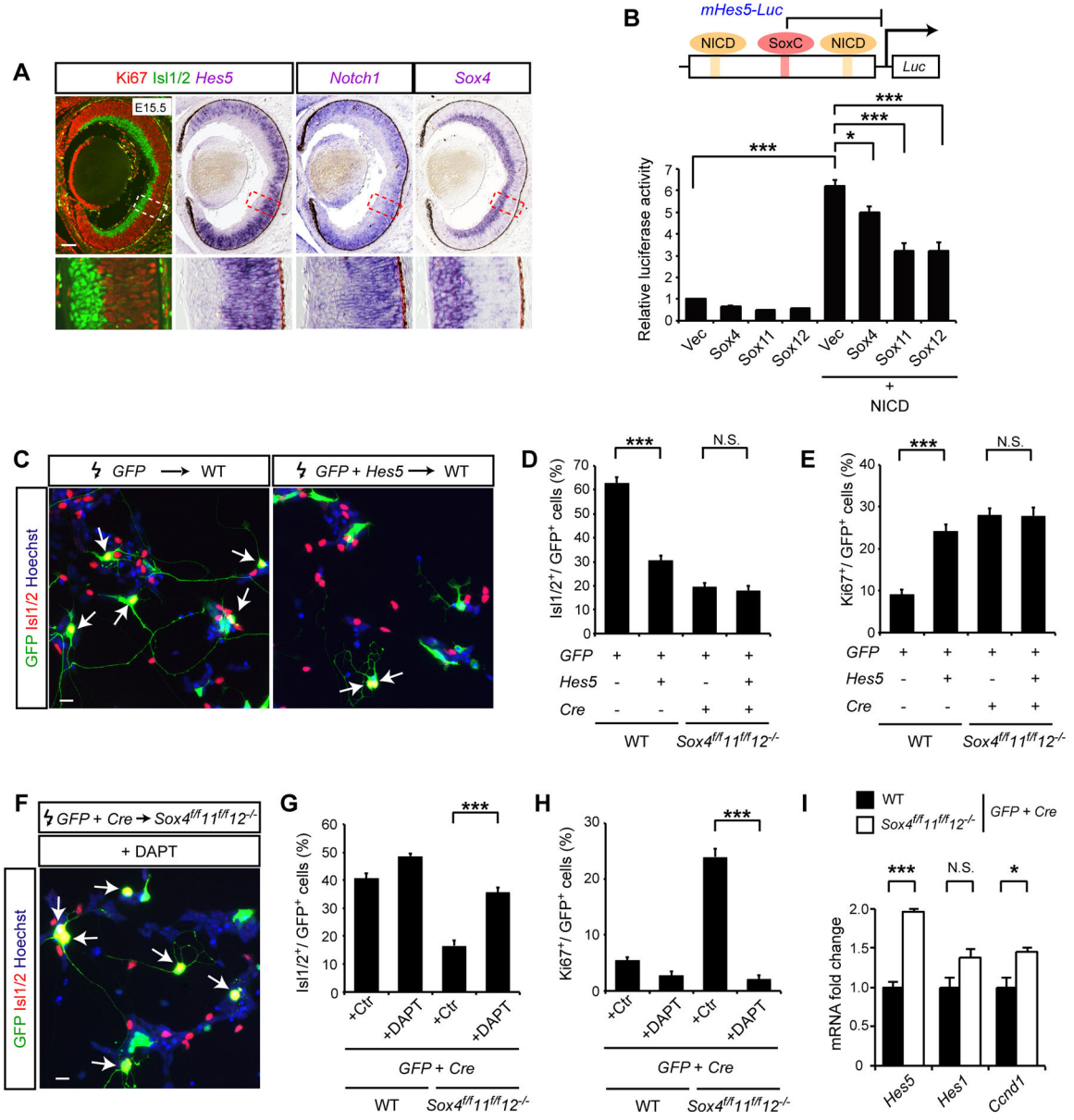

Figure 3. SoxC TFs repress Notch-Hes5 signaling to promote contralateral RGC differentiation

(A) Expression of *Hes5* and *Notch1* mRNAs in Ki67^{+} progenitor cells and *Sox4* mRNA in Islet1/2^{+} RGCs at E15.5. (B) Luciferase assay in HEK293 cells transfected with combinations of expression vectors for the Notch intracellular domain (NICD) (1.2 μg) and/or SoxC (4, 11, 12) (2.4 μg) with a reporter vector including the mouse *Hes5* promoter region (0.4 μg) and a *Renilla* luciferase construct (0.03 μg). Data are presented as fold change in relative luciferase activity normalized to the mean of empty vector (Vec). n = 4, two-way ANOVA. (C) Representative images of Islet1/2^{+} RGCs after overexpression of *CAG-Hes5* plasmid into WT DT retina (arrows). (D, E) Quantification of Islet1/2^{+}/GFP^{+} cells (%) (D) and Ki67^{+}/GFP^{+} cells (%) (E) in WT or *Sox4*$^{-/-}$*Sox11*$^{-/-}$*Sox12*$^{-/-}$ DT retina when Hes5 is overexpressed.(>360 of total GFP^{+} cells counted for each condition, n = 4, one-way ANOVA) (F) A representative image of Islet1/2^{+} RGCs in

Sox4$^{-/-}$*Sox11*$^{-/-}$*Sox12*$^{-/-}$ DT retinal cells with DAPT added to the medium (+ DAPT) (arrows). (G, H) Quantification of Islet1/2^{+}/GFP^{+} cells (%) (G) and Ki67^{+}/GFP^{+} cells (%) (H) in WT or *Sox4*$^{-/-}$*Sox11*$^{-/-}$*Sox12*$^{-/-}$ DT retinal cells cultured with control or DAPT (>370 of total GFP^{+} cells counted for each condition, n = 4 – 5, one-way ANOVA). (I) qRT-PCR measurements of *Hes5*, *Hes1*, and *Ccnd1* mRNAs of WT and *Sox4*$^{-/-}$*Sox11*$^{-/-}$*Sox12*$^{-/-}$ GFP^{+} cells. n = 4, Student's t test. See also Figures S3 and S4. Scale bars: 100 μm in B; 10 μm in C and F. * $p<0.05$, ** $p<0.01$, *** $p<0.001$, N.S. not significant.

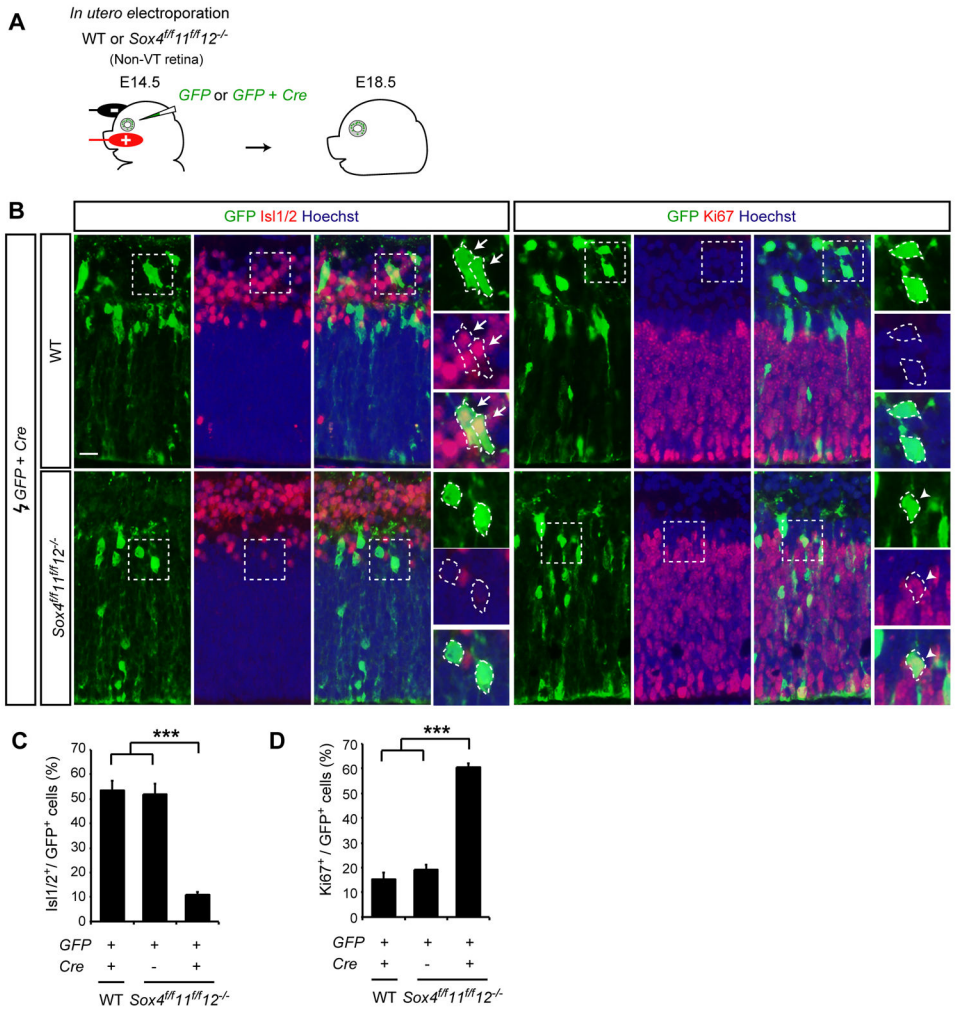

Figure 4. Contralateral RGC differentiation is impaired in SoxC mutant cells *in vivo*

(A) Schema of *in utero* retinal electroporation of *CAG-GFP* and *CAG-Cre* plasmids into E14.5 WT or $Sox4^{f/f}Sox11^{f/f}Sox12^{-/-}$ non-VT retina and analysis of RGC differentiation in central retina at E18.5. (B) Most E18.5 WT GFP^+ retinal cells have differentiated into $Islet1/2^+$ postmitotic RGCs (arrows in high magnification views), while many $Sox4^{-/-}Sox11^{-/-}Sox12^{-/-}$ GFP^+ retinal cells remain as $Ki67^+$ progenitor cells (arrowheads). (C, D) Quantification of $Islet1/2^+/GFP^+$ cells (%) (C) and $Ki67^+/GFP^+$ cells (%) (D) in WT, $Sox12^{-/-}$ and $Sox4^{-/-}Sox11^{-/-}Sox12^{-/-}$ non-VT retina (>2000 of total GFP^+ cells counted for each condition, n = 4 – 5, one-way ANOVA). Non-VT, non-ventrotemporal. Scale bar: 20 μm. *** $p<0.001$.

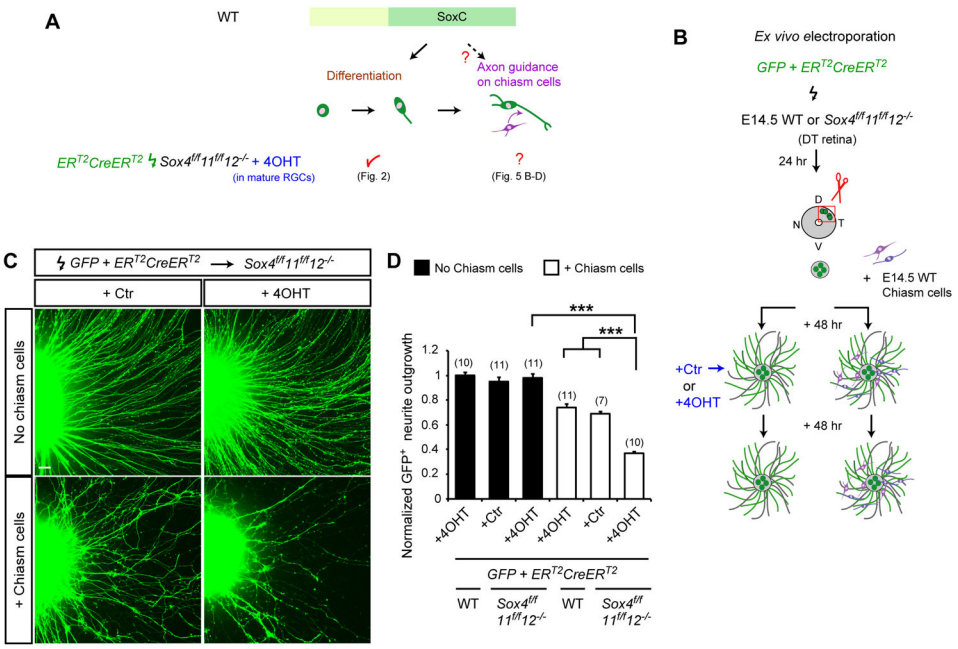

Figure 5. SoxC TFs are important for contralateral RGC axon outgrowth on chiasm cells

(A) Schema of hypothesis that SoxC TFs mediate axon guidance in response to signals from chiasm cells: after electroporation of *CAG-ER^{T2}CreER ^{T2}* into *Sox4$^{f/f}$Sox11$^{f/f}$Sox12$^{-/-}$* retina, retinal explants are treated with 4OHT only after RGC outgrowth has occurred (B–D). (B) Schema of *ex vivo* electroporation of *CAG-GFP* and *CAG-ER^{T2}CreER^{T2}* plasmids into E14.5 *Sox4$^{f/f}$Sox11$^{f/f}$Sox12$^{-/-}$* DT retina to generate *Sox4$^{-/-}$Sox11$^{-/-}$Sox12$^{-/-}$* GFP^{+} neurons by 4OHT in differentiated RGCs with neurites. (C) Representative images of *Sox12$^{-/-}$* or *Sox4$^{-/-}$Sox11$^{-/-}$Sox12$^{-/-}$* GFP^{+} axon outgrowth with or without chiasm cells. (D) Quantification of WT, *Sox12$^{-/-}$* or *Sox4$^{-/-}$Sox11$^{-/-}$Sox12$^{-/-}$* GFP^{+} DT retinal outgrowth in the presence or absence of chiasm cells. (n) = number of explants for each condition, two-way ANOVA. See also Figures S5 and S6. DT, dorsotemporal. Scale bars: 40 μm. *** p<0.001.

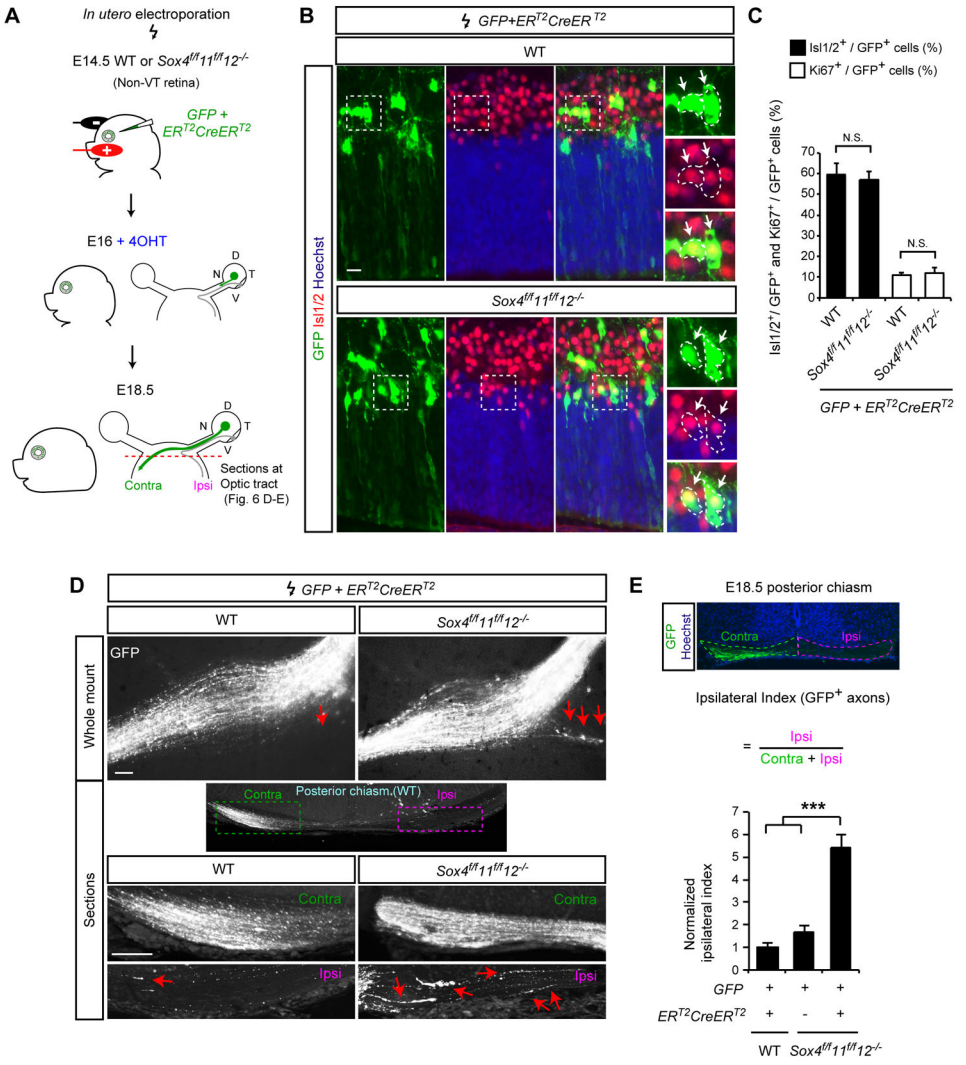

Figure 6. SoxC TFs mediate contralateral RGC axon projection at the chiasm midline

(A) Schema of *in utero* retinal electroporation of *CAG-GFP* and *CAG-ER^{T2}CreER^{T2}* plasmids into E14.5 WT or *Sox4$^{f/f}$Sox11$^{f/f}$Sox12$^{-/-}$* central retina, injection of 4OHT i.p. at E16, and analysis of RGC differentiation and retinal axon decussation at E18.5. (B) Most E18.5 WT GFP$^+$ retinal cells and *Sox4$^{-/-}$Sox11$^{-/-}$Sox12$^{-/-}$* GFP$^+$ retinal cells have differentiated to Islet1/2$^+$ postmitotic RGCs (arrows). (C) Quantification of Islet1/2$^+$ and Ki67$^+$/GFP$^+$ cells (%) in WT and *Sox4$^{-/-}$Sox11$^{-/-}$Sox12$^{-/-}$* retina (>870 of total GFP$^+$ cells counted for each condition, n = 3, two-way ANOVA). (D) A whole mount view of the GFP$^+$ axon projection from electroporated retina to the optic chiasm, and 300 μm chiasm sections after tissue clearing with *Clear^{T2}* (Sections) in WT and *Sox4$^{-/-}$Sox11$^{-/-}$Sox12$^{-/-}$* mutants. Arrows indicate axons projecting ipsilaterally. (E) Quantification of GFP$^+$ ipsilateral projection from WT, *Sox12$^{-/-}$* or *Sox4$^{-/-}$Sox11$^{-/-}$Sox12$^{-/-}$* non-VT retina. n = 4 – 6, one-way ANOVA. Schematic shows the measurement of pixel intensity of contralateral and ipsilateral optic tracts and the calculation to obtain an ipsilateral index. See also Figures S7 and S8. Non-VT, non-ventrotemporal. Scale bars: 20 μm in B; 100 μm in D. *** p<0.001. N.S. not significant.

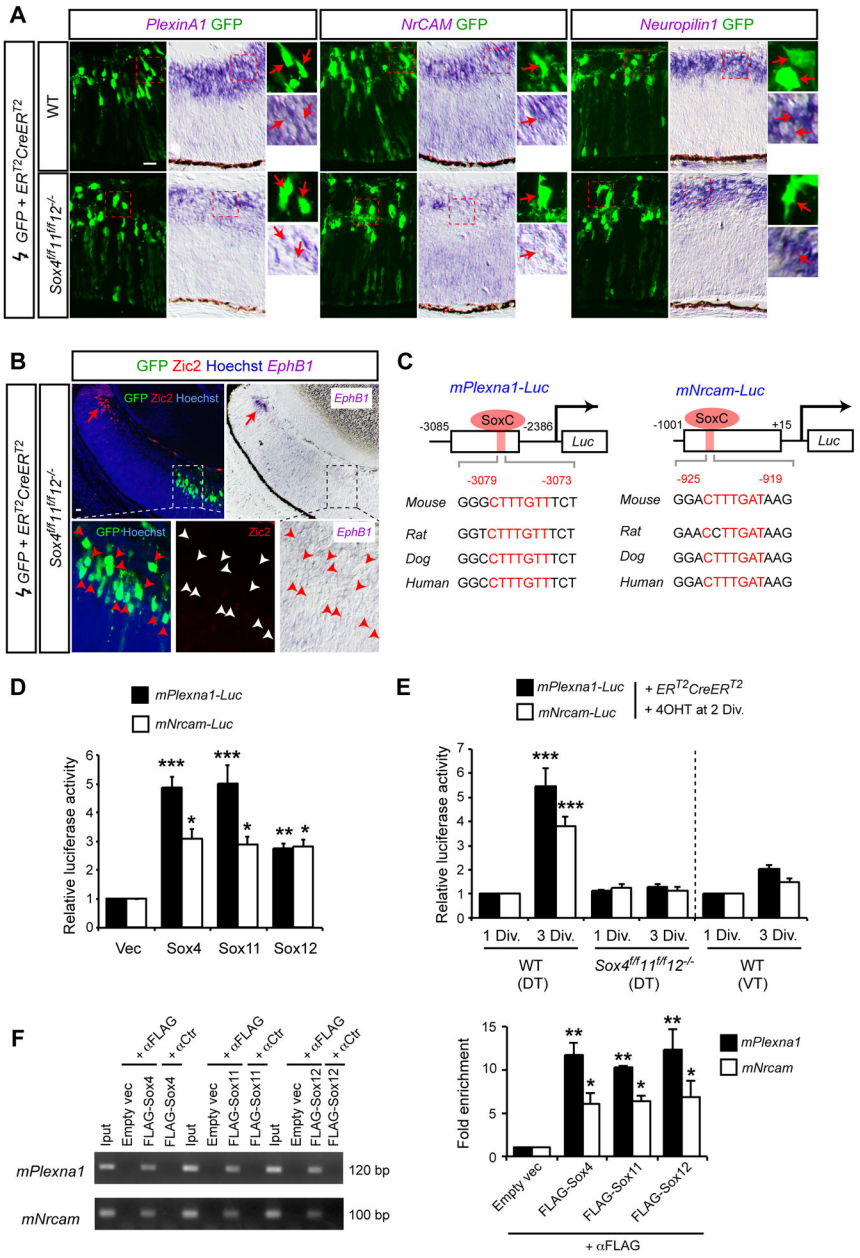

Figure 7. *Plexna1* and *Nrcam* are targets of SoxC TFs

(A, B) Expression of *Plexin-A1, Nr-CAM* and *Neuropilin1* mRNAs (A), and Zic2 protein and *EphB1* mRNA (B) in E18.5 WT or *Sox4*$^{-/-}$*Sox11*$^{-/-}$*Sox12*$^{-/-}$ GFP^{+} cells in central retina. Note that *Sox4*$^{-/-}$*Sox11*$^{-/-}$*Sox12*$^{-/-}$ display little expression of *Plexin-A1* and *Nr-CAM* mRNAs, while *Neuropilin1 mRNA* is unaffected (arrows)(A). Zic2 protein and *EphB1* mRNA were detected in VT retina (arrows), but not in *Sox4*$^{-/-}$*Sox11*$^{-/-}$*Sox12*$^{-/-}$ GFP^{+} cells (arrowheads) (B). (C) Conserved Sox-binding sites in *Plexna1* and *Nrcam* 5'-non coding region among binocular species and construction of luciferase-based reporter vectors. (D, E) Luciferase assay: HEK293 cells were transfected with combinations of expression vectors for SoxC (4, 11, 12) (3.6 μg) with reporter vector (0.3 μg) and a *Renilla* luciferase construct

(0.03 μg) (D). 0.5 μl of DNA solution of *GFP* (0.5 μg/μl), $ER^{T2}CreER^{T2}$ (2.0 μg/μl) and reporter vector (0.5 μg/μl) with a *Renilla* luciferase construct (0.05 μg/μl) was electroporated into E14.5 WT or $Sox4^{f/f}Sox11^{f/f}Sox12^{-/-}$ contralateral (DT) or ipsilateral (VT) retina. Dissociated retinal cells were cultured for 1 or 3 days or incubated with 4OHT for 1 day and analyzed (E). Data are presented as fold change in relative luciferase activity normalized to the mean of empty vector (Vec) (D) or WT (WT, 1 Div.) (E). n = 3 – 5, two-way ANOVA (D) and three-way ANOVA (E) . (F) Chip assay in DT retina, which was electroporated with FLAG-tagged Sox4, Sox11, Sox12 or empty vector and cultured. The *Plexna1* and *Nrcam* promoter sequences were amplified by PCR using input DNA (1% of total sample) and total immunoprecipitated DNA with FLAG antibody. The fold enrichment was quantified after ChIP assay with FLAG antibody. n = 3 – 5, two-way ANOVA. DT, dorsotemporal; VT, ventrotemporal. Scale bars: 20 μm. * $p<0.05$, ** $p<0.01$, *** $p<0.001$

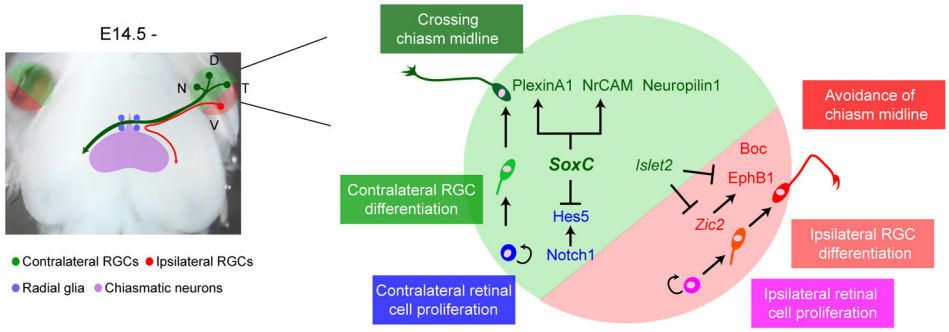

Figure 8. Functions of SoxC TFs in contralateral retina

SoxC TFs in non-VT retina promote contralateral RGC differentiation and axon guidance at the optic chiasm midline through interactions with their molecular targets, *Hes5*, *Plexna1* and *Nrcam*. In contrast, Zic2-EphB1 interactions mediate ipsilateral RGC axon projection and are repressed by Isl2, a TF for contralateral RGC axon guidance (Pak et al., 2004) and influenced by a cell adhesion molecule, Boc (Fabre et al., 2010; Sanchez-Arrones et al., 2013).